Old Dominion University
ODU Digital Commons

Electrical & Computer Engineering Faculty Publications | Electrical & Computer Engineering

7-2017

Perspective: The Physics, Diagnostics, and Applications of Atmospheric Pressure Low Temperature Plasma Sources Used in Plasma Medicine

M. Laroussi
Old Dominion University, mlarouss@odu.edu

Follow this and additional works at: https://digitalcommons.odu.edu/ece_fac_pubs

 Part of the Biomedical Commons, Biophysics Commons, and the Engineering Physics Commons

Repository Citation

Laroussi, M., "Perspective: The Physics, Diagnostics, and Applications of Atmospheric Pressure Low Temperature Plasma Sources Used in Plasma Medicine" (2017). *Electrical & Computer Engineering Faculty Publications*. 137.
https://digitalcommons.odu.edu/ece_fac_pubs/137

Original Publication Citation

Laroussi, M., Lu, X., & Keidar, M. (2017). Perspective: The physics, diagnostics, and applications of atmospheric pressure low temperature plasma sources used in plasma medicine. *Journal of Applied Physics, 122*(2), 020901. doi:10.1063/1.4993710

This Article is brought to you for free and open access by the Electrical & Computer Engineering at ODU Digital Commons. It has been accepted for inclusion in Electrical & Computer Engineering Faculty Publications by an authorized administrator of ODU Digital Commons. For more information, please contact digitalcommons@odu.edu.

Perspective: The physics, diagnostics, and applications of atmospheric pressure low temperature plasma sources used in plasma medicine

M. Laroussi, X. Lu, and M. Keidar

Citation: Journal of Applied Physics **122**, 020901 (2017); doi: 10.1063/1.4993710
View online: http://dx.doi.org/10.1063/1.4993710
View Table of Contents: http://aip.scitation.org/toc/jap/122/2
Published by the American Institute of Physics

Articles you may be interested in

Announcement: Journal of Applied Physics eliminates publication fees effective 1 June 2017
Journal of Applied Physics **122**, 010201 (2017); 10.1063/1.4989932

Active control and switching of broadband electromagnetically induced transparency in symmetric metadevices
Applied Physics Letters **111**, 021101 (2017); 10.1063/1.4993428

Tutorial: Reactive high power impulse magnetron sputtering (R-HiPIMS)
Journal of Applied Physics **121**, 171101 (2017); 10.1063/1.4978350

A diffuse plasma jet generated from the preexisting discharge filament at atmospheric pressure
Journal of Applied Physics **122**, 013301 (2017); 10.1063/1.4989975

Investigation of the properties of semiconductor wafer bonding in multijunction solar cells via metal-nanoparticle arrays
Journal of Applied Physics **122**, 023101 (2017); 10.1063/1.4992805

Application of coupled mode theory on radiative heat transfer between layered Lorentz materials
Journal of Applied Physics **121**, 183101 (2017); 10.1063/1.4983021

Perspective: The physics, diagnostics, and applications of atmospheric pressure low temperature plasma sources used in plasma medicine

M. Laroussi,[1,a)] X. Lu,[2] and M. Keidar[3]
[1]Plasma Engineering and Medicine Institute, Old Dominion University, Norfolk, Virginia 23529, USA
[2]State Key Laboratory of Advanced Electromagnetic Engineering and Technology, HuaZhong University of Science and Technology, Wuhan, Hubei 430074, People's Republic of China
[3]Mechanical and Aerospace Engineering Department, George Washington University, Washington DC 20052, USA

(Received 12 March 2017; accepted 3 June 2017; published online 13 July 2017)

Low temperature plasmas have been used in various plasma processing applications for several decades. But it is only in the last thirty years or so that sources generating such plasmas at atmospheric pressure in reliable and stable ways have become more prevalent. First, in the late 1980s, the dielectric barrier discharge was used to generate relatively large volume diffuse plasmas at atmospheric pressure. Then, in the early 2000s, plasma jets that can launch cold plasma plumes in ambient air were developed. Extensive experimental and modeling work was carried out on both methods and much of the physics governing such sources was elucidated. Starting in the mid-1990s, low temperature plasma discharges have been used as sources of chemically reactive species that can be transported to interact with biological media, cells, and tissues and induce impactful biological effects. However, many of the biochemical pathways whereby plasma affects cells remain not well understood. This situation is changing rather quickly because the field, known today as "plasma medicine," has experienced exponential growth in the last few years thanks to a global research community that engaged in fundamental and applied research involving the use of cold plasma for the inactivation of bacteria, dental applications, wound healing, and the destruction of cancer cells/tumors. In this perspective, the authors first review the physics as well as the diagnostics of the principal plasma sources used in plasma medicine. Then, brief descriptions of their biomedical applications are presented. To conclude, the authors' personal assessment of the present status and future outlook of the field is given. *Published by AIP Publishing.* [http://dx.doi.org/10.1063/1.4993710]

I. INTRODUCTION

Plasmas have been used for biological and medical applications for several decades. Some of these uses involved either low pressure plasmas[1,2] or relatively hot plasmas where thermal effects are dominant.[3] The low pressure work (mostly oxygen plasma) was partly conducted by NASA investigators aiming to destroy biological matter and inactivate microorganisms for space applications. Also, in the early 2000s, in-depth investigations of low pressure plasmas for medical sterilization applications were conducted by Moisan *et al.*[4] The thermal or "hot" plasma work mainly involved the use of plasma for cauterization and blood coagulation such as in the Argon Plasma Coagulator.[5]

In the late 1980s and early 1990s, engineering advances in the generation of large volume, low temperature, atmospheric pressure plasma took place. For simplicity and convenience, we refer to atmospheric pressure low temperature plasma as LTP throughout this paper. Investigators initially used the dielectric barrier discharge (DBD), powered by sinusoidal high voltages at kHz frequencies, and helium gas to produce relatively large volume diffuse plasmas.[6–8] The original aim was to use these plasmas for material processing, such as rendering plastics or cloth more hydrophilic or hydrophobic. However, by the mid-1990s, experiments were conducted that showed that these plasmas can also be used to inactivate bacteria.[9] This biological application attracted the attention of the Physics and Electronics Directorate of the US Air Force Office of Scientific Research (AFOSR) which saw the potential of using such plasmas to treat soldiers' wounds and sterilizing biotic and abiotic surfaces. Subsequently, the AFOSR funded proof of principle research work that started in 1997 and lasted for more than a decade. Parallel to this early work, efforts conducted in Russia showed that plasma-generated nitric oxide (NO) plays a crucial role in enhancing phygocytosis and accelerating the proliferation of fibroblasts. Both *in vitro* and *in vivo* experiments were conducted by the Russian investigators who called their approach "plasmadynamics therapy" of wounds.[10] Finally, and around 2002 researchers from the Netherlands reported that LTP can be used to detach mammalian cells without causing necrosis and under some conditions can even lead to apoptosis (programmed cell death).[11]

The above described groundbreaking early research efforts and later works by more investigators eventually led to the foundation of a novel multidisciplinary research discipline: the biomedical applications of low temperature plasma. Today laboratories from around the world form a sizable global research community working on understanding the interaction of LTP with biological cells, tissues, and systems. Figure 1 is a timeline graph showing some of the most important milestones in the development of the

a)Author to whom correspondence should be addressed: mlarouss@odu.edu

biomedical applications of LTP, a field known today as "plasma medicine."

The early experiments showed that the charged particles and the reactive oxygen and nitrogen species generated in the plasma can be transported to interact with biological cells and induce certain outcomes such as cell inactivation/death. However, as research in the biological and medical applications of plasma advanced a need for devices that can deliver plasma outside the confinement of electrodes and enclosures arose. This need was met by the development of plasma sources that are able to provide plumes of low temperature plasma outside the main discharge gap and into the ambient air. These devices are known as non-equilibrium atmospheric pressure plasma jets (N-APPJ).[12,13] To achieve biologically tolerable temperatures ($T < 40\,^{\circ}C$), various plasma jets were developed. For more details about these jets, the reader can consult Refs. 12–15. Most of these devices use noble gases, such as helium or argon as operating gas with or without admixtures of oxygen or air. Plasma plumes up to several centimeters in length can be achieved using DC, pulsed DC, RF, and even microwave power.[12]

In the presence of oxygen and nitrogen molecules, DBDs and N-APPJs are sources of copious amounts of reactive oxygen species (ROS) and reactive nitrogen species (RNS). Some of these reactive species, such as OH, O, $O_2(^1\Delta)$, O_2^-, H_2O_2, and NO, are known to have important biological implications. Recent investigations have shown that it is through these reactive molecules (radical and non-radical) that LTP affects prokaryotic and eukaryotic cells by upsetting the "equilibrium" of their redox processes and/or triggering cell signaling. For example, in the case of cancer, the mechanisms of action of LTP, which include the induction of apoptosis, cell cycle arrest at the S-phase, DNA damage/double-strand breaks, and increase of the intracellular ROS concentrations, are elicited via the ROS and RNS produced by the plasma. Therefore in the design and operation of LTP sources, it is of paramount importance to tailor the devices and the operating conditions to produce controllable levels of ROS and RNS in order to achieve the desired biological outcomes.

In this paper, the physics of the two main devices used in plasma medicine research to generate atmospheric pressure low temperature plasma is presented. These LTP sources are the dielectric barrier discharge (DBD) and non-equilibrium atmospheric pressure plasma jets (N-APPJ). Using advanced plasma diagnostics methods, measurements of important species of relevance to plasma medicine are presented. As an illustration of the use of LTP in medicine, brief highlights of various biomedical applications are covered. To conclude, the authors present their own general perspective of the present status and future of the field of plasma medicine.

II. DIELECTRIC BARRIER DISCHARGE

It was Theodose du Moncel who first discovered in 1853 that a discharge can be induced between two conducting plates separated by two glass plates.[16] To drive the discharge, he used a Ruhmkorff coil, which is an induction coil that allowed for the generation of high AC voltages from a low voltage DC source. Du Moncel's discovery was followed by the work of Werner von Siemens, who in 1857 reported on the design and application of a dielectric barrier discharge (DBD) to generate ozone.[17] Siemens' DBD apparatus had a cylindrical geometry with tin foils as electrodes and used glass as dielectric. However, it was only about 70 years later that serious scientific investigations to generate large volume non-equilibrium, low temperature, atmospheric pressure plasmas were carried out. These were conducted in the 1930s by Von Engel who tried to generate such plasma by controlling the temperature of the cathode (by water-cooling).[18] Such temperature control resulted only in marginal success with eventual occurrence of instabilities leading to plasma restrictions. Finally, and five decades after Von Engel's original trials, successful generation of relatively large volume, non-equilibrium, diffuse atmospheric pressure plasma was achieved (in the late 1980s and early 1990s). These successful experiments were first reported by Kanazawa *et al.*, Massines *et al.*, and Roth *et al.*[6–8] These investigators used the DBD configuration and applied sinusoidal voltages in the kV at frequencies in the kHz range. It is also of note to mention here the impressive work carried out by Kogelschatz and co-workers for the understanding of the physics of the DBD and its optimization for the generation of ozone.[19–21]

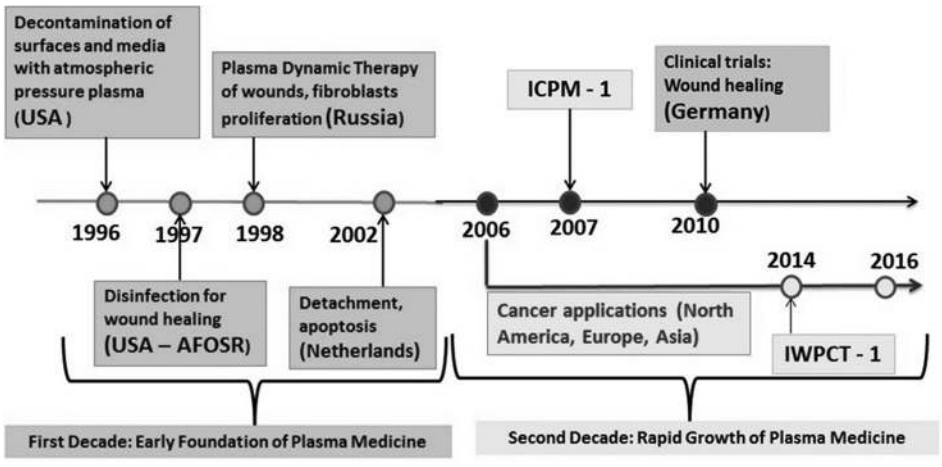

FIG. 1. Timeline showing the major early milestones of the field of plasma medicine. The first conference entirely dedicated to plasma medicine, the International Conference on Plasma Medicine (ICPM), was established in 2007. The first workshop entirely dedicated to the cancer applications of LTP, the International Workshop on Plasma for Cancer Treatment (IWPCT), was established in 2014.

The performance of the DBD was greatly improved upon when (late 1990s and early 2000s) fast rise time voltage pulses with pulse widths in the nanoseconds-microseconds range were employed. These pulses transfer the applied energy to the electron population and effectively allow a means to control the electron energy distribution function (EEDF). This control of the EEDF leads to the possibility of tailoring and enhancing of the plasma chemistry.[22–25] The DBD proved to be very relevant to various plasma processing applications and was the first device used in the mid-1990s in the early experiments on the biological applications of LTP.[9,26–28] These early experiments showed that the charged particles and reactive species generated in the plasma can be transported to interact with biological cells and induce certain biological outcomes.

DBDs use a dielectric material to cover at least one of the electrodes. The electrodes are driven by voltages of several kV at frequencies in the kHz range. DBDs usually generate plasmas with filamentary structures resulting in non-uniform material treatment. However, in the late 1980s and in the 1990s a quest to develop DBDs that can generate non-filamentary or diffuse plasma led to interesting results. Several reports were published that showed that under some conditions DBDs can produce diffuse, relatively homogenous plasmas, at atmospheric pressure.[6–8,29–32]

The geometry of DBDs usually consists of two planar or co-axial electrodes separated by an adjustable gap, with at least one of the electrodes covered by a dielectric material. Figure 2 shows a schematic of a DBD with a planar geometry.

A. Sinusoidal excitation

Under sinusoidal excitation, the electrodes of the DBD are energized by high sinusoidal voltages with amplitudes in the 1 to 20 kV range, at frequencies in the kHz range. The electrode arrangement is generally contained within a vessel to allow for the introduction and control of a gaseous mixture. Surface charges accumulate on the dielectric as soon as a discharge is ignited in the gas. These surface charges create an electrical potential, which counteracts the externally applied voltage, resulting in self-limitation of the discharge current. Although generally DBDs produce filamentary plasmas, under some conditions homogeneous plasmas can also be generated. The charge accumulation on the surface of the dielectric material covering the electrodes plays a crucial role in maintaining the non-equilibrium nature of the plasma.

Figures 3(a) and 3(b) show the current waveforms in the case of a filamentary discharge and a diffuse discharge, respectively. Filamentary discharges exhibit multiple current pulses per half cycle, while diffuse/homogeneous discharges exhibit a current waveform with a single wide pulse per half cycle. Using fast photography, Gherardi *et al.*[32] observed the structure of the discharge channel. As shown in Fig. 4(a), when the plasma is homogeneous, intensified charge-coupled device (ICCD) images show a luminous region extending uniformly over the entire surface of the electrode surface. However, when the plasma is filamentary, several localized discharges are clearly visible, as shown in Fig. 4(b). Other important discharge parameters for both types of discharges are: The electron density, n_e, and temperature, T_e, are in the 10^{14}–10^{15} cm^{-3} and 1–10 eV ranges inside a plasma filament, while n_e and T_e are in the 10^{9}–10^{11} cm^{-3} and 0.2–5 eV ranges for a diffuse discharge.

The operating conditions that lead to a diffuse plasma were originally suggested by Kanazawa *et al.*[6] These

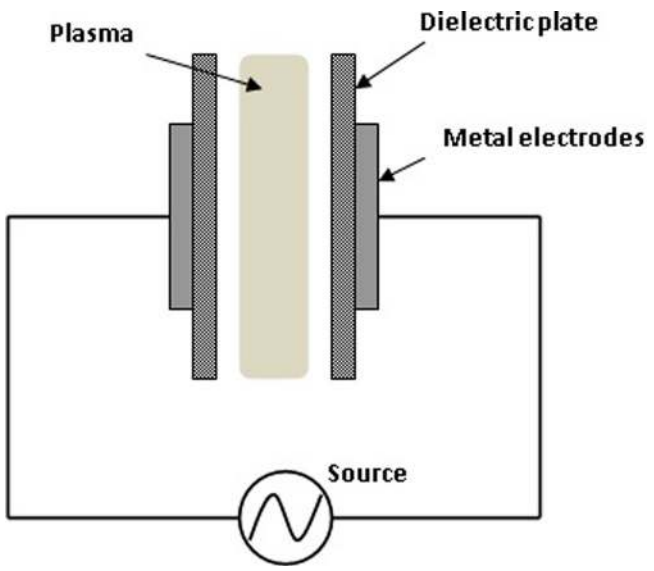

FIG. 2. Schematic of a dielectric barrier discharge with a planar geometry.

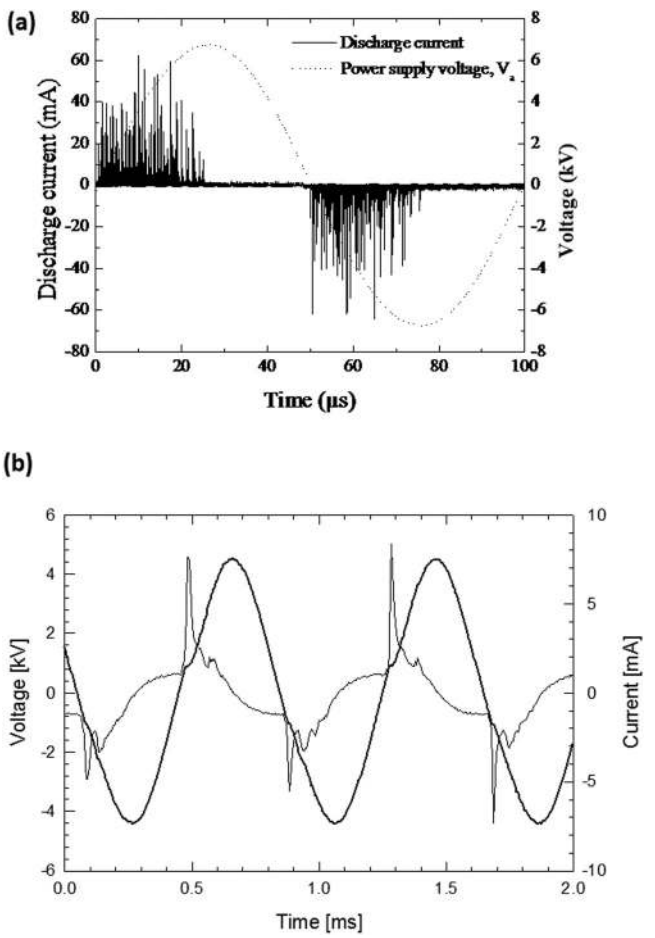

FIG. 3. Current-voltage characteristics of the dielectric barrier discharge. (a) Filamentary discharge; (b) Diffuse discharge.

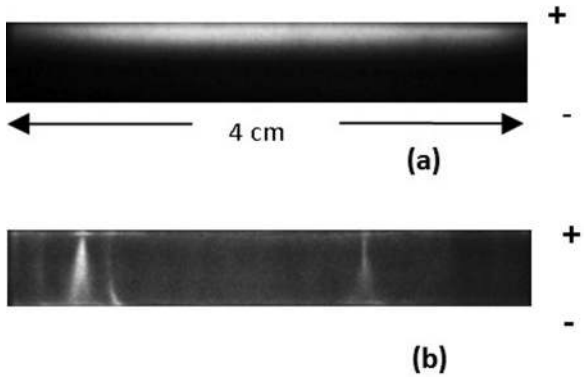

FIG. 4. ICCD images of a DBD in N_2. (a) Diffuse discharge; (b) Filamentary discharge. Exposure time: 10 ns.[32] Reproduced with permission from Gherardi *et al.*, Plasma Sources Sci. Technol. **9**, 340 (2000). Copyright 2000 Institute of Physics.

conditions are: 1. Helium used as the operating gas; 2. The frequency of the applied voltage must be in the kHz range. However, other investigators were able to generate diffuse plasmas with other gases and in different frequency ranges.[33–36] According to Massines *et al.*, the mechanisms that lead to a diffuse plasma are the following: Seed electrons and metastable atoms that can be available between current pulses make gas breakdown possible under low electric field conditions. These seed particles allow for either a Townsend-type breakdown or a glow discharge depending on the gas (nitrogen vs. helium). If helium is the gas used, a density of seed electrons greater than $10^6\,cm^{-3}$ was found to be sufficient to keep the plasma ignited under low field conditions.[32] The seed electrons are those left over from the previous current pulse and/or those produced by Penning Ionization. If nitrogen is used, it is the metastables that play the dominant role in keeping the discharge ignited between pulses. In this case, the surface of the dielectric, which can be a source of quencher species, plays an important role in setting the available concentration of metastable atoms.

To calculate the power deposited in the plasma generated by a DBD, the Lissajous method can be used. A capacitor (measuring capacitor) with a capacitance much larger than the DBD capacitance is connected in series with the DBD as shown in Fig. 5. A plot of the applied voltage, V_a, versus charge, Q, can then be drawn such that the area contained under the contour of the plot represents the dissipated power. Figure 6 is such an illustration. Numerically, the power calculation can be done this way: In order to calculate the power dissipated in the gas, the voltage across the gas gap is determined as

$$V_g = V_a - V_C, \tag{1}$$

where V_a is the applied voltage, and V_C is the voltage drop across the measuring capacitor C such as $V_C \ll V_a$. Note that in these calculations V_R is neglected since it is very small compared to V_C. The numerical integration for the power dissipated in the discharge is given by

$$P_{abs} = \frac{1}{T}\sum_n (V_a - V_C)\cdot\frac{Q}{t_n}\cdot(t_{n+1} - t_n). \tag{2}$$

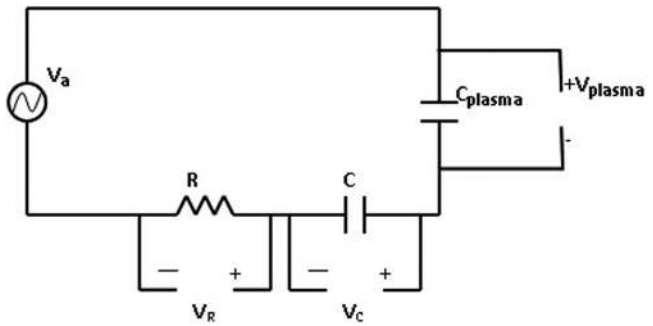

FIG. 5. Circuit allowing the measurement of the power dissipated by a DBD.

Here, the expression $Q = i.t$ is used to get $idt = (Q/t)\,dt$, and $Q = CV_C$ is used to calculate the charge Q from the voltage across the measuring capacitor, C.

B. Pulsed excitation

The electron energy distribution in non-equilibrium discharges plays the most important role in defining the chemistry in the plasma. It is through electron impact excitation and ionization that the charged particles, excited species, and radicals are produced. Increasing the electron number density and their energy translates to an increase in the production of reactive species. To achieve this increase of ionization and to extend the electron energy distribution to higher values, short high voltage pulses can be used. Pulses with widths less than the characteristic time of the onset of the glow-to-arc transition help keep the plasma stable and maintain its non-equilibrium nature. Figures 7 and 8 show plots of the EEDF for a sinusoidal and pulsed DBD, respectively.

Pulsed Dielectric Barrier Discharges (P-DBD) in xenon (pressure range 100–400 Torr) using a grid electrode configuration and in the helium/air mixture at atmospheric pressure with a planar electrode geometry were reported.[22,24,25] At

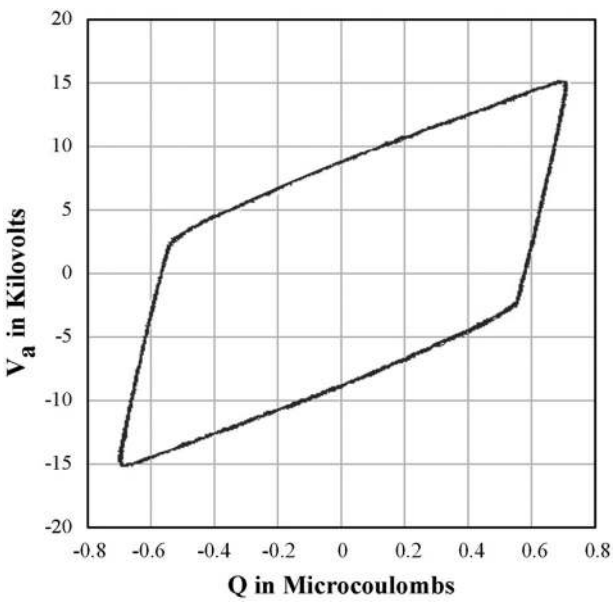

FIG. 6. Lissajous plot for a DBD allowing the calculation of the dissipated power in the discharge.

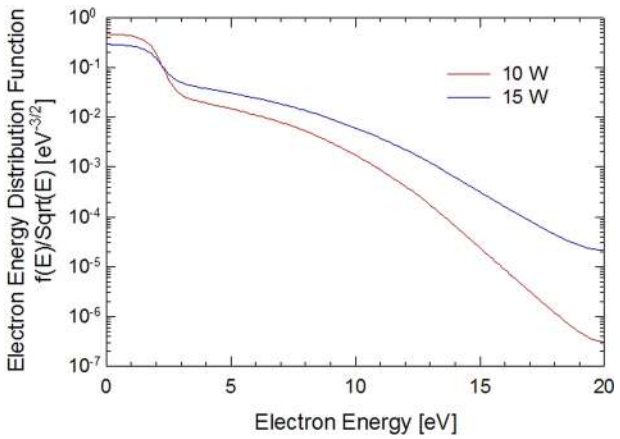

FIG. 7. Electron energy distribution function for a DBD driven by 3 kHz sinusoidal voltage (gas: air).

atmospheric pressure, the P-DBD generated large volume diffuse plasma in atmospheric pressure He, He/O_2, He/air, or He/N_2 mixture. The discharge was driven by sub-microsecond unipolar square pulses. Figure 9 shows a photograph of the discharge when helium is used as the operating gas. These investigators reported that two discharges occur for every applied voltage pulse.[24] The first discharge (or "primary" discharge) was ignited at the rising edge of the applied voltage pulse, while the second discharge (or "secondary" discharge) was self-ignited during the falling edge of the applied voltage pulse. Figure 10 shows the I-V characteristics of the discharge, and Fig. 11 shows ICCD images of the onset of the primary and secondary discharge.[25]

The power supplied to the discharge as well as the power dissipated/absorbed by the plasma can be calculated from the I-V characteristics. Figure 12 shows the total power supplied by

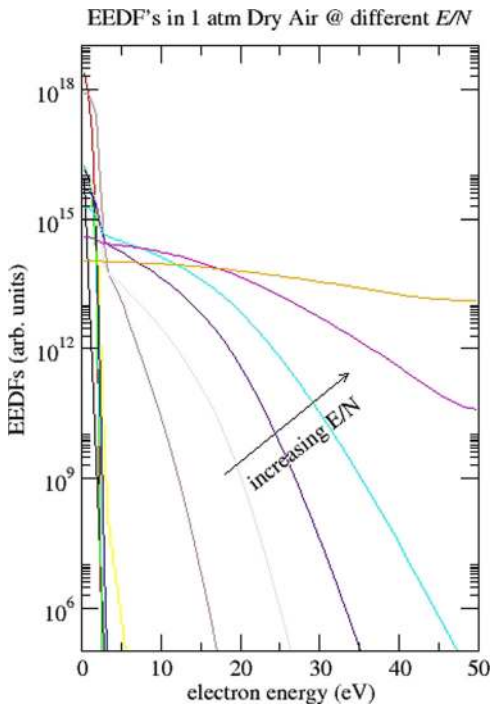

FIG. 8. Electron energy distribution function for a DBD driven by repetitive 500 ns high voltage pulses; gas is dry air (Courtesy: V. Kolobov).

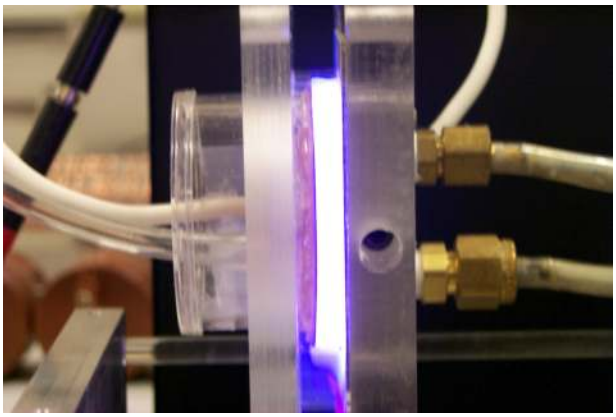

FIG. 9. Photograph of a diffuse P-DBD discharge. Gas: helium; Pulse width: 500 ns; Rep rate: 5 kHz.

the power supply, P_{supp}, and the power dissipated in the plasma, P_{gas}.[24] P_{supp} is the product of the total current, I_{tot}, and the applied voltage, V_a. P_{gas} is the product of the discharge current $I_{discharge}$ ($I_{discharge} = I_{tot} - I_{Displacement}$) and the voltage across the gas, V_g. During the rising front of the applied voltage, P_{supp} includes both the power dissipated in the plasma and the reactive power stored in the various system capacitors. The negative sign of P_{supp} represents a power returned to the power source. The curve representing P_{gas} shows the power dissipated in the plasma during the primary and the secondary discharge. It is of importance to note here that the secondary discharge occurs without any power contribution from the external power supply.[24]

The gas temperature in the pulsed DBD was estimated by analyzing the rotational structure of the N_2 second positive system emission and was found to be around 350 K. The N_2 rotational structure contains information on the rotational temperature. Because of the low energies needed for rotational excitation and the short transition times, molecules in the rotational states and the neutral gas molecules are in equilibrium. Therefore, the gas temperature can be directly inferred from the rotational temperature. To determine the gas temperature, the experimentally measured spectra are compared with simulated spectra of the 0–0 band of the second positive system of nitrogen. Figure 13 is an illustration

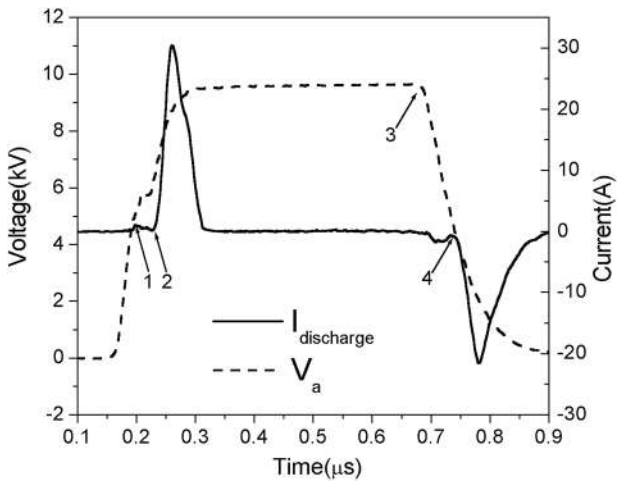

FIG. 10. Current-voltage characteristics of a P-DBD in helium.[24]

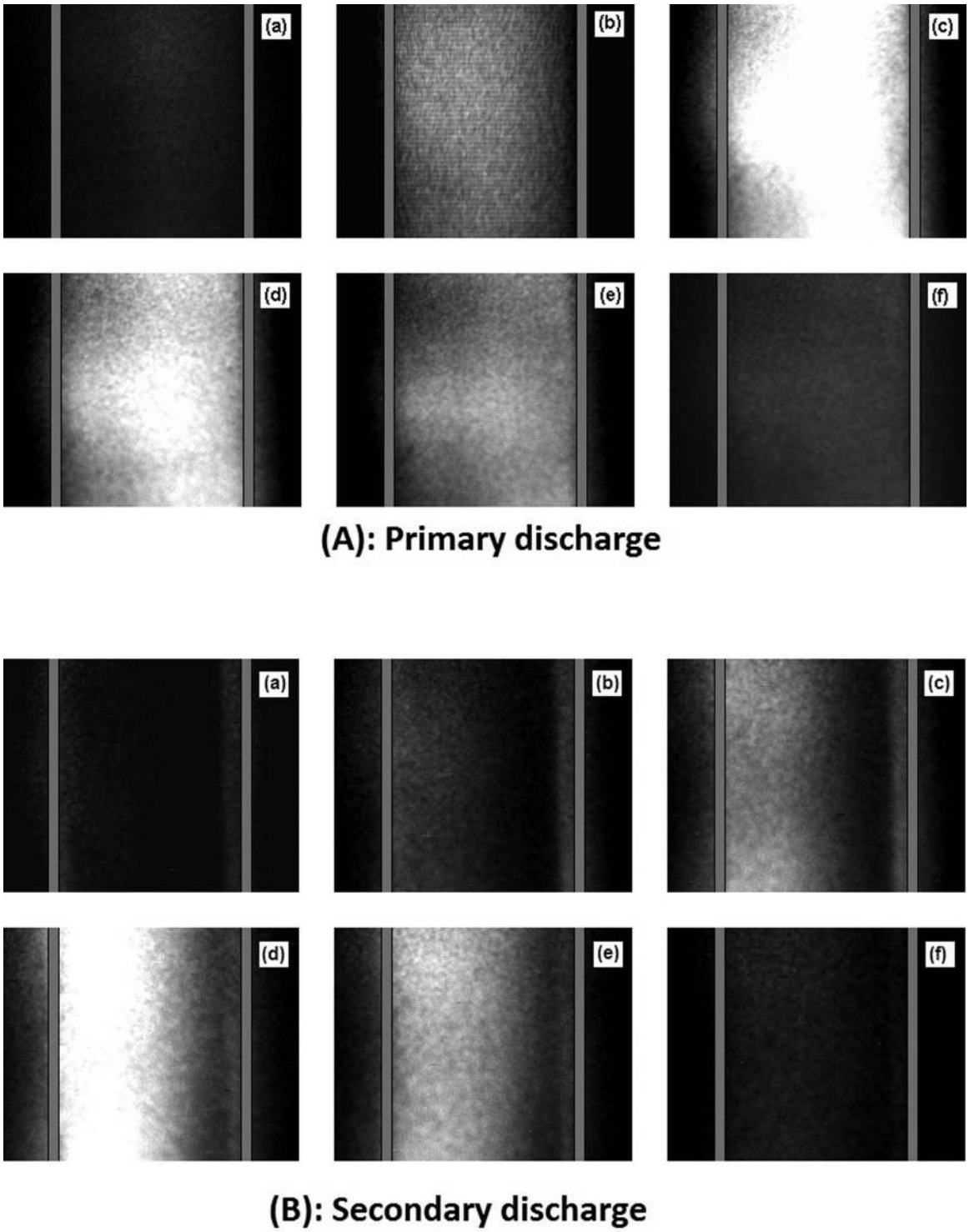

FIG. 11. ICCD images of the P-DBD in helium (exposure time: 5 ns). (A) Primary discharge occurring at the rising edge of the voltage pulse: (a) 0 ns, (b) 5 ns, (c) 20 ns, (d) 30 ns, (e) 40 ns, and (f) 70 ns; (B) Secondary discharge occurring at the falling edge of the voltage pulse: (a) 515 ns, (b) 520 ns, (c) 525 ns, (d) 540 ns, (e) 550 ns, and (f) 585 ns.[25] Reproduced with permission from Lu and Laroussi, J. Phys. D: Appl. Phys. **39**, 1127 (2006). Copyright 2006 Institute of Physics.

of the temperature measurement method explained above for the case of the P-DBD.[25]

III. NON-EQUILIBRIUM ATMOSPHERIC PRESSURE PLASMA JETS (N-APPJS)

Non-equilibrium atmospheric pressure plasma jets have the unique characteristic to produce plasmas that propagate away from the confinement of electrodes and into the ambient air. The plasma can therefore be delivered to a target located remotely from the plasma generation area. This characteristic makes N-APPJs very attractive tools in various novel applications including in biology and medicine.[37–43] Various power driving methods that include pulsed DC, RF, and microwave power have been used.[12] Investigators have

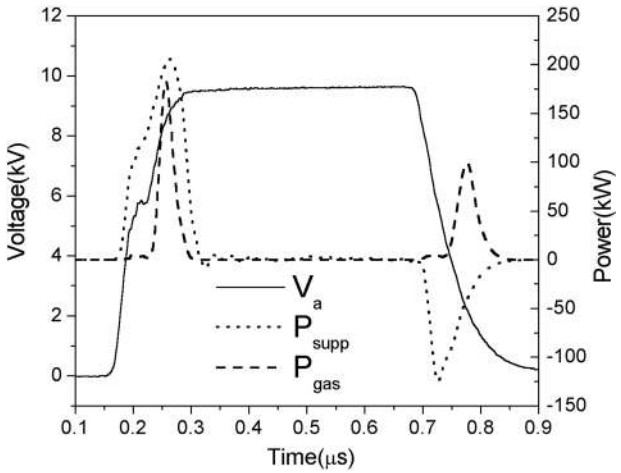

FIG. 12. Applied voltage, supply power, P_{supp}, and gas dissipated power, P_g, versus time. When P_{supp} is positive, the power is supplied from the source to load, and when P_{supp} is negative, the power is restored from the load to source.[24]

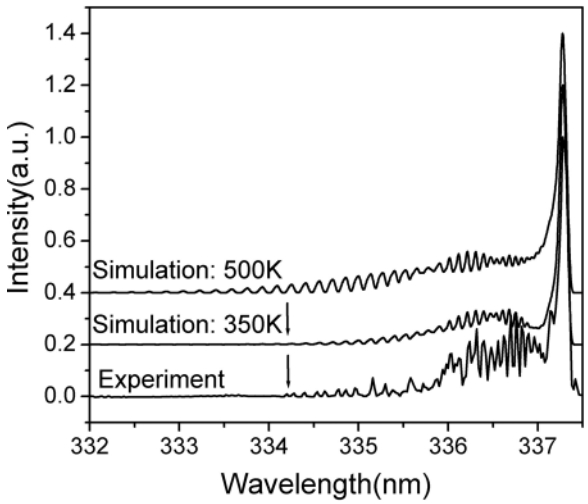

FIG. 13. Experimental and simulation spectra of N_2 second positive 0-0 transition. The applied voltage =9 kV, pulse frequency =1 kHz, pulse width =500 ns, gap distance =2 mm, and operating gas mixture gas: He(90%) + N_2(10%).

also developed various electrode configurations ranging from a single electrode, to two ring electrodes wrapped around the outside wall of a cylindrical dielectric body, to two ring electrodes attached to centrally perforated dielectric disks. Figure 14 shows three typical examples of N-APPJ configurations.[13] Noble gases such as helium and argon have been used as operating gases, usually at flow rates in the 3–10 slm range. Admixtures of air or oxygen can be added to these background gases. Depending on the power applied, the gas type, and flow rate, stable plasma plumes with lengths up to several centimeters have routinely been generated.

Because the plasmas generated by N-APPJs are launched in air, they provide very interesting reactive chemistry that can be exploited in various plasma processing applications. Reactive oxygen species (ROS), such as O, OH, and O_2^-, and reactive nitrogen species (RNS), such as NO and NO_2, are abundantly produced. These reactive species have important

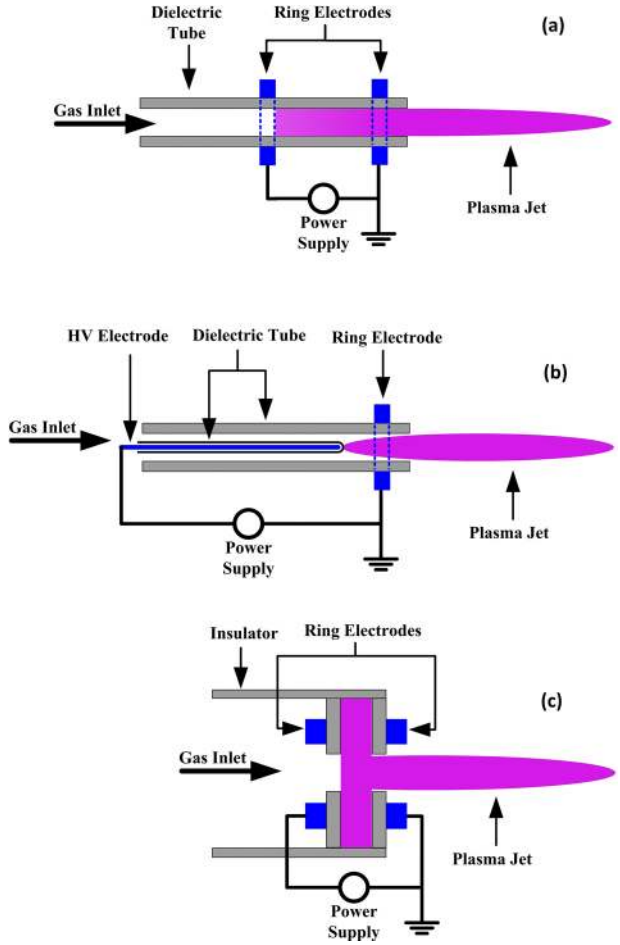

FIG. 14. Schematic of three typical N-APPJ configurations. (a) Two ring electrodes wrapped around the outer surface of a cylindrical dielectric tube; (b) A central needle-like electrode and an outer ring electrode; (c) Two ring electrodes attached to two centrally perforated dielectric disks.[13]

biological implications such as the inactivation of pathogenic bacteria and the destruction of cancer cells.[38–43]

A. Propagation of the plasma plume

In the mid-2000s, investigators reported that plasma jets are not continuous volumes of plasma but are made of small plasma packets propagating at high velocities of up to 10^5 m/s.[44,45] These fast propagating plasma packets came to be known as "plasma bullets." Subsequent to this discovery, extensive experimental and modeling work by various groups has elucidated the physical mechanisms governing the generation and propagation of these plasma bullets.[46–62] Lu and Laroussi first proposed a photoionization model to explain the dynamics of the plasma bullet.[45] But further investigations, including modeling and simulation, showed that the high electrical field present at the head of the bullet plays a crucial role in the generation and the propagation processes of the plasma bullets. The strength of the electric field was experimentally measured by various investigators and was found to have an average value in the 10–25 kV/cm range:[63–65] Using the intensity ratio method of the nitrogen first negative system at 391.4 nm and second positive system at 337.1 nm, Begum *et al.*[63] measured a local electric field of

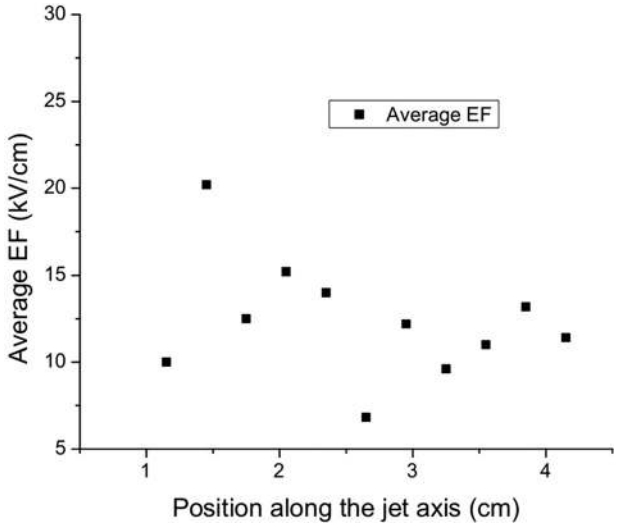

FIG. 15. Average electric field at the head of the plasma bullet.[63]

up to 95 kV/cm. These same authors, using a dielectric probe, reported an average field of 24 kV/cm.[52] Stretenovic *et al.*[64] used the Stark polarization spectroscopy method to measure electric fields in the 10–20 kV/cm range, depending on the plasma jet source (in helium) configuration. Sobota *et al.*[65] used a method based on the Pockels technique on a birefringent dielectric material (BSO crystal, $Bi_{12}SiO_{20}$) and measured a maximum field of 11 kV/cm. Figure 15 shows the average electric field as measured by an electric probe.[63]

The current carried in the plasma plume was also measured using a Pearson coil through which the plasma plume was threaded. Figure 16 shows the jet current waveform versus time at various locations along the axis of propagation.[58] Based on ICCD imaging, electric field measurements, and discharge current measurements (I-V characteristics), it was concluded that the plasma bullets are the product of fast ionization waves. These ionization waves are guided within the gas channel, hence the name "Guided Ionization Waves."[66]

Measurements of the velocity of the plasma bullets were conducted using three different methods: electrical, fast imaging, and spectroscopic methods.[58] Figure 17 shows a spatially resolved measurement of the bullet velocity and

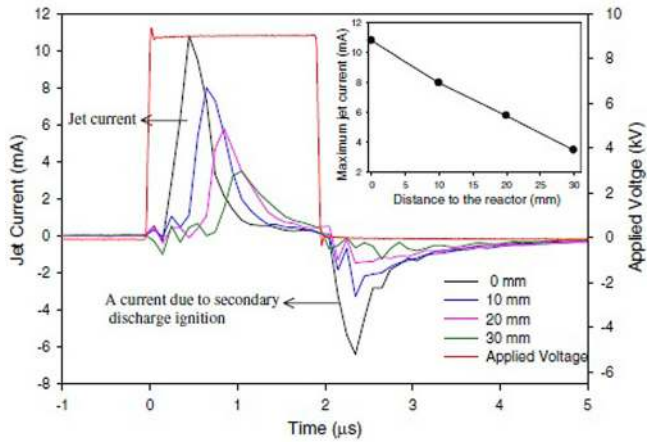

FIG. 16. Jet current versus time measured at different axial locations along the plasma jet. Gas: helium at 5 slm; Pulse width: 2 μs.[58]

temporally resolved fast images of the plasma bullet corresponding to each propagation phase. Three different phases can be defined: A launching phase exhibiting increasing velocity, a propagation phase where the bullet velocity is first relatively constant then undergoes a slow decay, and finally an ending phase where the bullet slows down.

B. Structure of the plasma bullets

Using head-on fast photography, Mericam-Bourdet *et al.* were able to show that the plasma bullets leave the jet nozzle with a hollow/ring structure (donut, ring shape).[46] Modeling work by Sakiyama *et al.*[60] supported this observation. The ring-like structure of the plasma bullet can be visually observed due to the emission coming from excited species at the boundary between the flowing gas channel and the ambient air. There, reactions between metastable helium and nitrogen lead to Penning type ionization. As the plasma bullet travels away from the jet nozzle and due to air diffusion, the molar fraction of helium relative to that of air falls below a threshold value. When this happens, it leads to plasma quenching and collapse of the ring shape, ultimately leading to the end the bullet propagation.[51] Figure 18 is an illustration of the annular shape of the plasma bullet.

IV. REACTIVE SPECIES OF RELEVANCE TO PLASMA MEDICINE AND THEIR DIAGNOSTICS

Mounting experimental evidence has shown that LTP interacts with biological cells and tissues mostly via the reactive species it produces. These include reactive oxygen species (ROS) and reactive nitrogen species (RNS). It is well known from cell biology that both ROS and RNS play important biological roles in cell function but can also have cytotoxic effects that can be detrimental to the cell. For example, the hydroxyl radical (OH), which is produced by plasma as it interacts with air moisture, causes peroxidation of unsaturated fatty acids which are a major component of the lipids constituting the cell membrane. Another byproduct of plasma application is hydrogen peroxide (H_2O_2). Hydrogen peroxide possesses strong oxidative properties that affect, via the peroxide ions, lipids, proteins, and DNA. In the presence of nitrites, H_2O_2 can react to form peroxynitrite. Interaction of peroxynitrite with biological cells leads to either caspase activation followed by apoptosis or to lipid peroxidation, protein nitration, or oxidation, which can result in necrosis. Nitric oxide (NO) is another species that can be generated by plasma as it interacts with air. The NO molecule is known to have several biological effects which include the regulation of immune-deficiencies, induction of phagocytosis, proliferation of keratinocytes, and regulation of collagen synthesis. Therefore, it is of the utmost importance to quantitatively measure the concentrations/fluxes of all reactive species known to play potential roles when LTP interacts with biological matter.

Sections IV A–IV C briefly present various diagnostics techniques used in LTP studies to determine important plasma parameters such as gas temperature, electron density, electric field, and chemical species concentrations. In addition and as illustrative cases, we present experimental

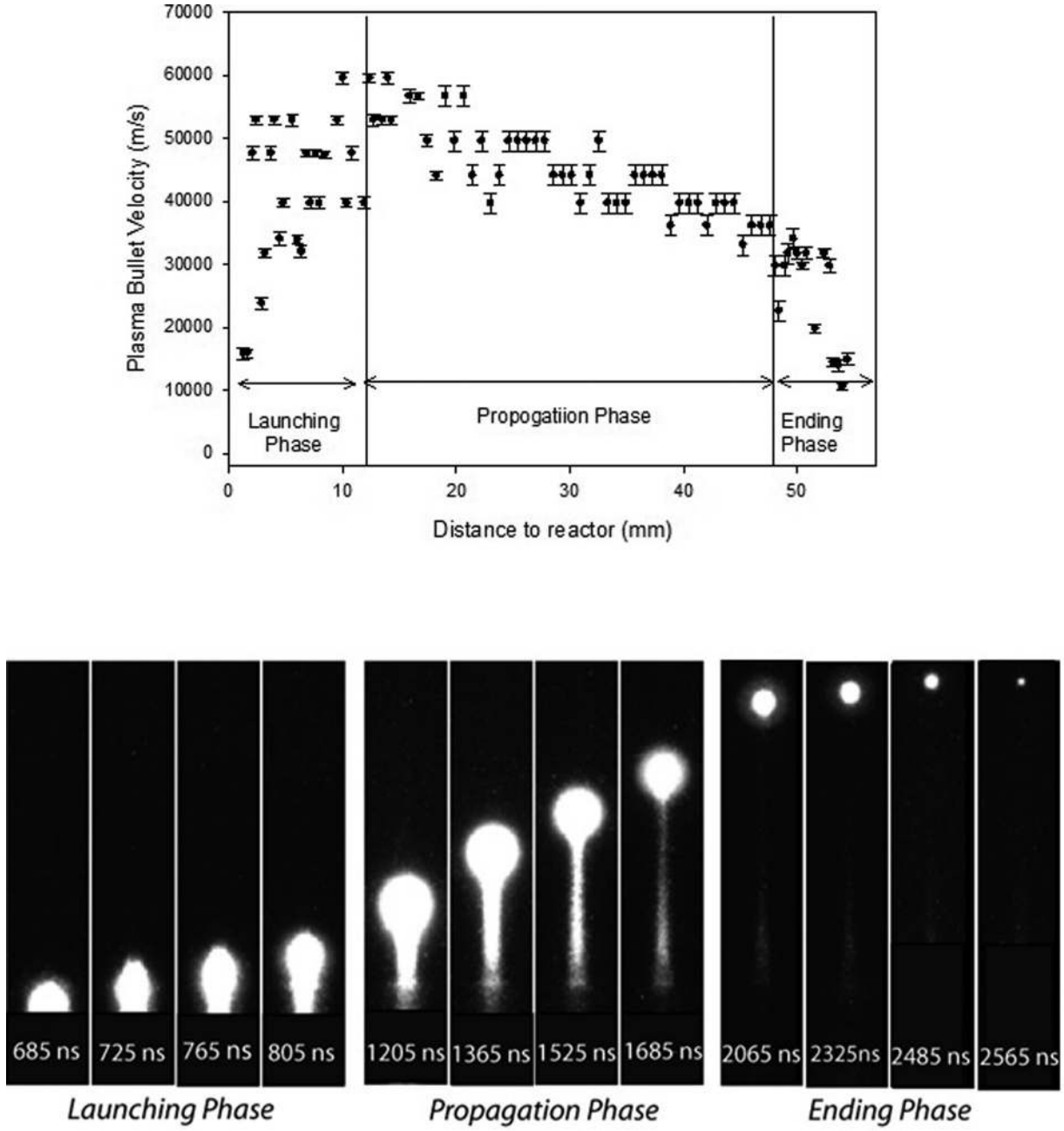

FIG. 17. Plasma bullet velocity versus axial distance showing the three propagation phases (Top figure). The lower figure shows ICCD images of the plasma bullet corresponding to the three propagation phases. Gas: helium at 5 slm; Pulse width: 2 μs.[58]

measurements of hydroxyl, OH, and atomic oxygen, O. For extensive measurements, under various plasma operating conditions, of many other relevant species (such as $O_2(^1\Delta)$, O_2^-, NO, and others) the reader can consult Ref. 67.

A. Diagnostics for atmospheric pressure low temperature plasmas

Because most of the atmospheric pressure low temperature plasmas have relatively small dimensions and significant non-uniformity, invasive techniques with low spatial resolution are not suitable as they yield incorrect mean values and significantly disturb the plasma properties. Non-invasive optical diagnostic techniques are thus the methods of choice for the diagnostics of atmospheric pressure low temperature plasmas. These techniques include optical emission spectroscopy (OES), laser induced fluorescence (LIF), two photons LIF (TALIF) techniques, scattering techniques such as Rayleigh-, Raman-, and Thomson scattering, and optical absorption spectroscopy measurements (VUV to MIR) and cavity ring down spectroscopy. Other commonly used techniques are known from chemical analysis such as mass spectrometry, gas chromatography or electron paramagnetic resonance spectroscopy, and some others. Details about these techniques can be found in Ref. 67.

In this paper, only several mature diagnostic techniques that were widely applied are introduced, which are OES, LIF, and TALIF. As we will discuss in the following, under

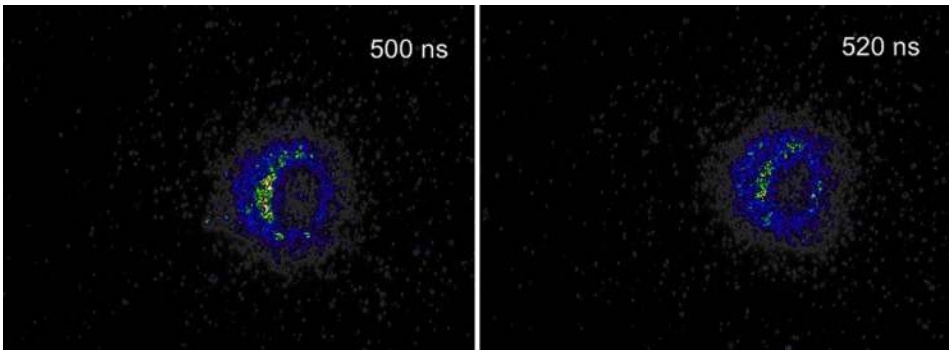

FIG. 18. ICCD images illustrating the ring-shaped structure of the plasma bullet as it leaves the nozzle of the plasma pencil.[46] Reproduced with permission from Mericam-Bourdet *et al.*, J. Phys. D: Appl. Phys. **42**, 055207 (2009). Copyright 2009 Institute of Physics.

certain conditions, OES could be used to obtain several of the most important plasma parameters, including the electron density, electron temperature, electric field, and so on. On the other hand, OH and O, two of the reactive species that play important roles in various biomedical applications, could be measured by laser induced fluorescence (LIF) and two photons LIF (TALIF), respectively. Details of these techniques will be discussed in Sections IV B and IV C.

1. Optical emission spectroscopy

Optical emission spectroscopy (OES) is probably one of the most widely used diagnostics for low temperature plasma. This is due to the nature of plasmas, which emit light in a broad spectrum, from vacuum ultraviolet to infrared. OES offers a non-intrusive diagnostics technique with spatial resolution up to micrometer and temporal resolutions up to nanosecond. By using OES, some of the important plasma parameters can be determined such as gas temperature, vibrational temperature, electron temperature, electron density, types of reactive species, and even absolute concentrations of some reactive species.

In general, OES can be classified into two categories, i.e., relative OES and absolute OES. According to their literal meanings, relative OES means measuring the relative optical emission intensity, while absolute OES means measuring the absolute optical emission intensity. The latter needs calibration and thus is more complicated. Besides, even with absolute OES, to know the absolute concentration of the corresponding excited species, assumptions on the excitation and de-excitation are still needed to know the absolute concentration of the excited species. Because of this, only few studies have been reported on absolute OES diagnostic on low temperature plasma for biomedical applications. Therefore, absolute OES will not be further discussed in this paper. On the other hand, even with relative OES, various plasma parameters can still be measured. Furthermore, it is worthy to emphasize that optical emission measures the light emitted from an excited state, but not from the ground state, which could have much higher concentrations and play more important roles in various applications. On the other hand, with certain assumptions and modelling, it is also possible to estimate the absolute concentration of certain species in the ground state by using OES. In Sections IV A 2–IV A 5, the OES technique for measuring different plasma parameters will be discussed.

2. Gas temperature and vibrational temperature

For molecular gases, in each electronic level there are several vibrational levels and for each vibrational level there are several rotational states. Using OES to measure gas temperature has been applied for low temperature plasma. In order to determine the background gas temperature, the simulated spectra of a selected band, often 0–0 band, of the second positive system of N_2 are compared with the experimental results. Because of the low energies needed for rotational excitation and the short transition times, molecules in the rotational states and the neutral gas molecules are in equilibrium. Consequently, the rotational temperature provides also the value of the gas temperature. It needs to be pointed out that when rotation bands of other molecular emission, such as OH (A-X) emission, are present, the gas temperature of a plasma could be significantly different from the rotational temperature obtained from OH (A-X) emission. This is because, in order to have the rotational states and the neutral gas molecules in equilibrium, the rotational energy transfer (RET) time constant needs to be significantly smaller than the effective radiative lifetime of OH(A), which is reduced significantly to the same order of rotational energy transfer time (about 1 ns), it could result in the non-Boltzmann rotation population distributions and the rotational population distribution does not have sufficient time to obtain thermal equilibrium. As a result, the gas temperature would be different from the rotational temperature.[68] However, under some circumstances, the rotational population distribution could be simplified as two temperatures,[69–72] such as shown in Fig. 19

Similarly, the OES is also often used to obtain the vibrational temperature of low temperature plasma when several vibrational bands can be detected. The vibrational temperature is typically hundreds or thousands of Kelvin indicating that vibrational levels are not highly populated at ambient temperatures. Again, the second positive system of N_2 is widely used to obtain the vibrational temperature of low temperature plasma for biomedical applications.

3. Electron temperature

For low temperature plasma, according to the electron energy distribution function, the number of the low energy electrons is often much higher than that of the high energy electrons. So the bound electrons on the high excited levels could be in collisional equilibrium with the free electrons

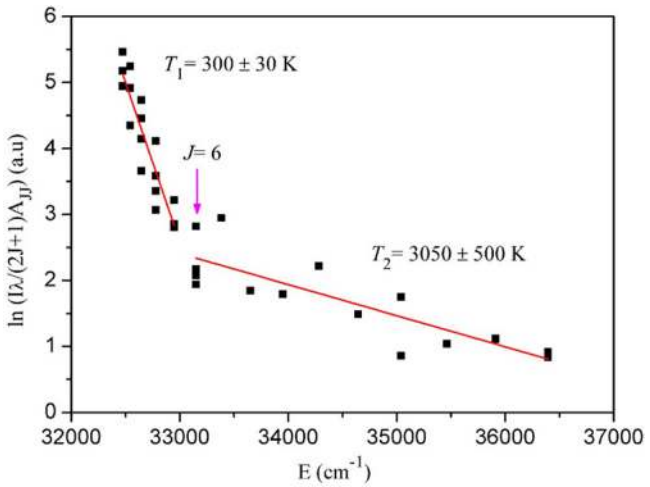

FIG. 19. Boltzmann plot of the OH(A-X) band transition in an Ar plasma plume.[69] Reproduced with permission from Xiong *et al*., J. Phys. D: Appl. Phys. **43**, 415201 (2010). Copyright 2010 Institute of Physics.

because the energy difference between the high excited levels and the ionization energy is small. Thus, they could satisfy the Boltzmann law because they experience a much greater number of inelastic collisions than the electrons on the lower levels. One of the frequently used examples is the emission from the excited states of 4p and 5p of Ar lines. The populations of the electrons on the lower excited levels normally do not satisfy the Boltzmann law because they are not in collisional equilibrium with the free electrons.[73,74]

To see if the Boltzmann law is applicable or not, the logarithm of the population concentration of the excited levels as a function of their energy, with reference to the ground state, is plotted, which is called a Boltzmann curve. If the law is satisfied, a straight line is obtained, proportional to excitation temperature T_{exc}^{-1}.

4. Electron density

The electron density is one of the most important parameters because it regulates the physics and chemistry of the plasma. Only a few measurements have been, however, carried out on the electron density of atmospheric pressure low temperature plasmas used for biomedical applications. Some traditional methods used for measurements of the electron density in low-pressure plasmas are not applicable for atmospheric low temperature plasmas. For instance, using a Langmuir probe may be difficult as its theory in a collision-dominant atmospheric pressure condition is not well developed, in addition to its finite size. The Stark broadening spectroscopic method by exploring the lineshape of the Balmer β transition (4–2) of atomic hydrogen at 486.132 nm enables the derivation of electron density only when it is higher than $5 \times 10^{13}\,cm^{-3}$ because of the large pressure broadening superposed over the Lorentzian shape.[75]

For low temperature Ar plasma, when the electron density is higher than $10^{15}\,cm^{-3}$, the Stark effect of Ar line broadening plays an important role and can be used for the purpose of electron density diagnostics.[76–78] Besides the Stark broadening, the spectral line emitted from the plasma can be broadened by other mechanisms, such as the Doppler and the van der Waals effects. The broadening induced by the instrument, the natural, and resonance broadening is negligible for most cases. In addition, it is noteworthy to emphasize that the line broadening also depends the electron density as shown in Fig. 20.

The microwave scattering technique was proposed by Shneider and Miles for measurements of electron density in small plasmas.[79] This method is well suited for plasma jets. Electron motion in atmospheric plasmas is heavily affected by collisions with gas atoms and restoration force from ions on electrons. Rayleigh scattering on the plasma electrons becomes the dominant component in the scattered signal due to significantly stronger polarizability of plasmas compared to that of molecules. Using the calibrated microwave scattering technique, plasma density in the streamer channel of about $10^{13}\,cm^{-3}$ was reported.[80,81]

5. Electric field

The electric field is another important parameter that can play a role in biomedical applications. For atmospheric pressure low temperature plasma, any intrusive method will disturb the electric field distribution. Optical emission spectroscopy is one of the potential methods used for the measurement of the

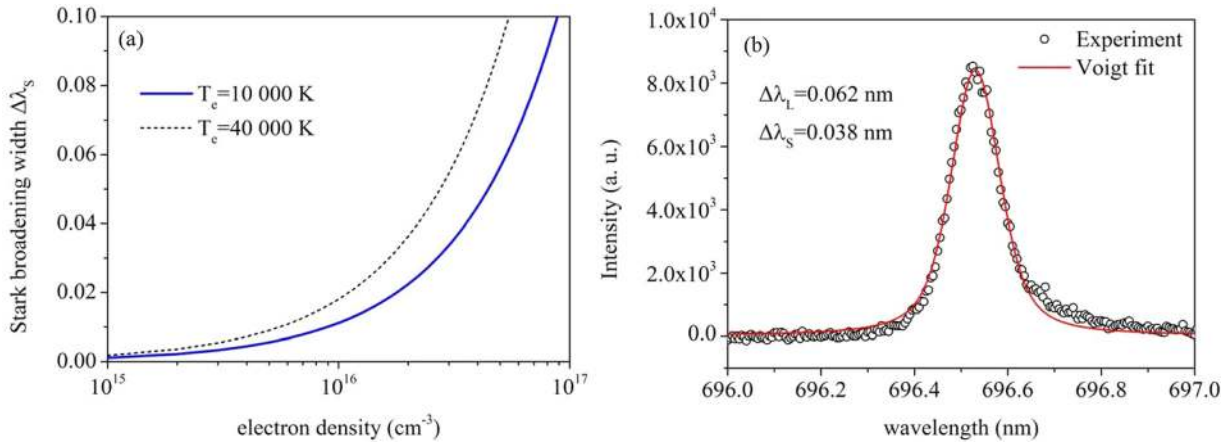

FIG. 20. (a) The relationship between the Stark broadening width and the electron density for T_e = 10 000 K and T_e = 40 000 K. (b) Voigt fitting of the Ar 696.5 nm line profile of the microplasma.[78]

electric field under certain conditions, based on the application of the polarization-dependent Stark splitting and shifting of He 447.1 nm line, and its forbidden counterpart. This technique requires relative wavelength shift measurements only. In order to obtain the electric field of the plasma, the relationship between the displacement of He energy sublevels and the electric field needs to be evaluated, which is well-established by investigators such as Foster.[82] The Stark components arising from transitions between sublevels with magnetic quantum numbers $m = 0$ and $m = 1$ of both allowed and forbidden lines are practically unresolvable for most setups. In addition, the π ($\Delta m = 0$) components are usually stronger than σ ($\Delta m = \pm 1$) components. The mutual wavelength separation $\Delta\lambda$ can be evaluated by taking an average value for m: 0–0 and 1–1 transition and the results can be fitted with the following polynomial:

$$\Delta\lambda = -1.06 \times 10^{-5} \cdot E^3 + 5.98 \times 10^{-4} \cdot E^2 + 2.57 \times 10^{-4} \cdot E + 0.1479. \quad (3)$$

Figure 21 shows the corresponding $\Delta\lambda$ for electric field from 0 to 20 kV/cm and Fig. 22 shows an example of electric field in an atmospheric pressure plasma plume.[83]

B. Laser Induced Fluorescence (LIF)

As discussed above, optical emission spectroscopy (OES) by itself can only measure the concentrations of species in excited states. However, for atmospheric pressure low temperature plasmas, most of the reactive species might be in the ground states. Laser-induced fluorescence (LIF) is perfect for measuring the concentrations of the reactive species in the ground states. LIF is based on a two-step process. In the first step, molecules or atoms in the electronic initial state $|1\rangle$ are excited to an upper electronic state $|3\rangle$ by absorbing one laser photon with energy $h\nu_{13}$. In the second step, $|3\rangle$ undergoes spontaneous radiative decay to a lower state $|2\rangle$, and the corresponding $h\nu_{32}$ photon is the spectroscopic observable called the fluorescence signal. With calibration of

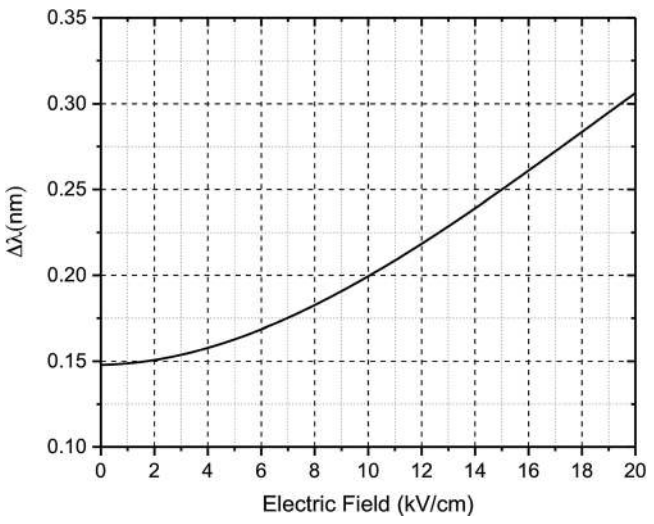

FIG. 21. The polynomial best fit of the calculated wavelength separation $\Delta\lambda$ of π components of the 447.1 lines from Eq. (3).

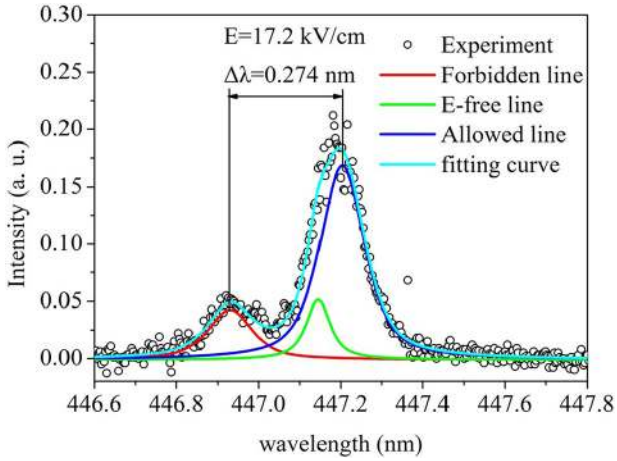

FIG. 22. π-polarized spectra of the He 447.1 nm line of an atmospheric pressure plasma plume.[83]

species having a known concentration and similar energy levels and similar excitation coefficients or by fitting the LIF signal decay with consideration of the quenching paths, the concentrations of the species concentration in the ground states can be obtained.

However, when molecules rather than atomic species are to be measured the technique is more complex. As an example let's discuss the case of the OH radical, which plays an important role in biomedical applications. The OH $A^2\Sigma^+$-$X^2\Pi$ band system has been widely applied to the measurement of the OH(X) concentration in different atmospheric low temperature plasma sources. The amount of fluorescence reflects the fraction of molecules promoted to the excited state which undergo radiative decay back to the ground stare. Such decay behavior is influenced by a number of factors, including the rates for spontaneous emission and for collisional energy transfer processes such as quenching, vibrational energy transfer (VET), and rotational energy transfer (RET). Therefore, in OH molecular LIF experiments, the observed fluorescence is comprised of different spectral emissions from different excited levels due to the VET and RET processes induced by collisions with the surrounding species. The VET and RET in the upper state act to redistribute the population from the laser excited level to other rovibrational states. The well-known approaches for the LIF signal interpretation employed for direct absolute radical concentration calculations, i.e., the so-called "three level model," which assumes that the molecules excited to the upper state remain in the original excited level until spontaneous emission, is not valid for plasma at high pressure. The spontaneous transitions from the laser excited level of OH($A^2\Sigma^+$) compete with these fast processes which transfer the molecule to a different rotational state within the same vibrational manifold (rotational energy transfer, RET) or to a different vibrational level (vibrational energy transfer, VET) and these processes result in the generation of additional rovibrational emission bands in the LIF spectrum. Therefore, a complex function of pressure, temperature, and chemical composition, and the distribution of OH molecules throughout the large manifold of rovibrational energy levels determine the detected broadband LIF signal. Details about how

to obtain the OH(X) concentration from LIF for atmospheric pressure low temperature can be found in Refs. 84–91.

Furthermore, for atmospheric pressure plasma jet, one of the widely used LTP sources for biomedical applications, because of the gas flow, the OH loss mechanisms are even more complicated than the static discharge (no gas flow) because gas flow can blow the OH generated in the upstream to the downstream thus resulting in the redistribution of the OH radicals.

As shown in Fig. 23, when the gas flow effect is considered in the model, a better fit between the experimental data and the simulated decay curve can be achieved when the initial OH density is $2.4 \times 10^{13}\,\mathrm{cm}^{-3}$. According to Fig. 5, it can be concluded that the OH lifetime under those experimental conditions is on the order of millisecond. Because of this relatively longer lifetime, the OH concentration should increase after each discharge pulse after the first discharge and saturate after a certain number of pulses.

C. Two photon absorption LIF (TALIF)

The single-photon absorption LIF scheme is possible if an optically allowed electronic transition is available for the $|i\rangle$ state to be probed, with a wavelength within the range of a tunable lasers. The possibility of absorption can be extended by multiphoton absorption, in particular, two-photon absorption, in which the final level $|j\rangle$ is reached through an intermediate level $|\mathrm{int}>$ in a two-step process (see Fig. 24). $|\mathrm{int}\rangle$ can be a virtual level or a real stationary electronic state. In the first case, the LIF technique is referred to as TALIF and in the second case OODR-LIF.[93]

As an example, let us discuss TALIF used for the measurement of the concentration of atomic oxygen, O. As illustrated in Fig. 8, a laser beam at 225.62 nm is used for exciting the transition of O $2p^4{}^3P_2 - 3p^3{}^3P_2$. The fluorescence at about 845 nm corresponding to the transition of O $3p^3P_2 - 3s^3S$ is captured by an ICCD camera. In order to calibrate the absolute O concentration, xenon is widely used. A UV beam at 224.24 nm is generated by a Dye Laser for

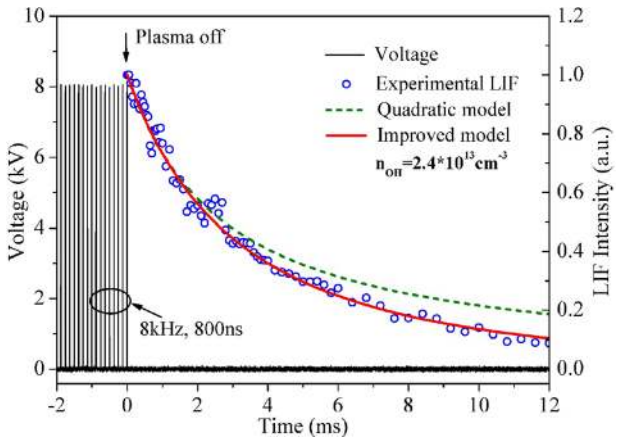

FIG. 23. Characteristic decay curve of the OH LIF signal. The blue circle is the experimental LIF signal. The red solid line is the simulation result from the improved model, which considers the gas flow effect.[92] Reproduced with permission from Pei *et al.*, IEEE Trans. Plasma Sci. **42**, 1206 (2014). Copyright 2014 Institute of Electrical and Electronics Engineers.

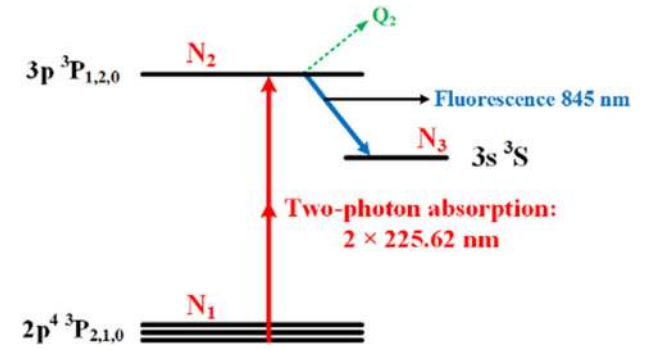

FIG. 24. Energy transfer process of O atom TALIF measurement.

stimulated transition Xe $5p^6\ ^1S_0 - 6p'[3/2]_2$. Then, the spontaneous transition Xe $6s'[1/2]_1 - 6s'[1/2]_1$ with fluorescence at about 835 nm is captured. Comparing the captured emission intensity of these transitions, absolute O concentration can be estimated according to the known concentration of Xe.[94–96]

Figure 25 shows the temporally resolved TALIF signal as a function of time between pulses for the case of a pulsed plasma jet when 0.9% of O_2 is premixed with helium and a shielding gas of dehumidified nitrogen is used. The O concentration drops slightly during the pulse cycle of 125 μs, which indicates that the life time of O atom is much longer than 125 μs.[94]

D. Summary

As reviewed in Ref. 67, the OH concentrations of plasma jets reach up to the order of $10^{13}/\mathrm{cm}^3$ for pulsed jets driven (rep rate of 20 kHz), $10^{14}/\mathrm{cm}^3$ for jets driven by a RF power, and $10^{15}/\mathrm{cm}^3$ for jets driven by a microwave power. Similarly, the O concentrations of plasma jets reach up to the order of $10^{14}/\mathrm{cm}^3$ for jets driven by a RF power, and $10^{16}/\mathrm{cm}^3$ for jets driven by microwave power. In addition, the electrode configuration, the gas composition, the surrounding gas and its humidity, and whether an object/target is placed in front of the plasma jet (including the object's characteristics, such as wetness, roughness, and conductivity) all could

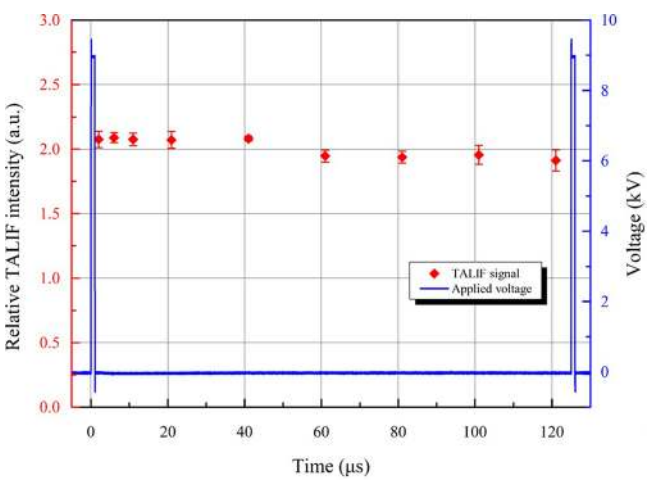

FIG. 25. Time-resolved atomic O TALIF signal of an atmospheric pressure plasma jet during one pulse period. Working gas: premixing 0.9% O_2 with helium. Shielding gas: N_2.[97]

affect significantly the reactive species distributions and concentrations.

V. BIOMEDICAL APPLICATIONS OF ATMOSPHERIC PRESSURE LOW TEMPERATURE PLASMAS

The unique chemical and physical properties of LTP technology have enabled its recent biomedical applications including sterilization, polymer material preparation, wound healing, tissue or cellular removal, dental treatment, and cancer therapy. It is becoming increasingly evident that the advantages of LTP are due to the production and efficient delivery of reactive oxygen and nitrogen species, RONS, analogous to those naturally produced by cells.[27,40,98–100] Thus, LTP is capable of gentle non-thermal modification of the radical balance in cells leading to apoptosis rather than necrosis. In Sections V A–V E, brief reviews of select applications of LTP in biology and medicine are presented, starting with cancer applications which are experiencing remarkable advances.

A. LTP in cancer therapy

Recent research indicates that LTP selectively eradicates brain tumor cancer cells *in vitro* without damaging normal cells and significantly reduces tumor size *in vivo*. These results indicate that LTP can lead to a new paradigm in cancer therapy by offering a minimally invasive surgery technique which allows specific cell removal without affecting the entire surrounding tissue. Reactive oxygen and nitrogen species (ROS/RNS) metabolism and oxidative stress-responsive genes are shown to be markedly regulated in tumor cells in response to LTP treatment.[101] It is envisioned that this technology could be adapted for clinical use and would fundamentally enhance treatment of brain tumors. The main goal of anti-cancer therapies ("Holy Grail") has been to selectively kill cancer cells without damaging the normal cells of that tissue, i.e., maximize the therapeutic outcome for the cancer patients. Normal cells were shown to be less sensitive to the effects of LTP treatment than cancer cells, supporting the notion that LTP treatment is likely to play a pivotal role as an anti-cancer therapeutic tool.

Since the first report about the killing effect of DBD on melanoma in 2007, the field of LTP application in cancer treatment experienced a fast growth (Fig. 26). To date, LTP treatment has demonstrated its significant anti-cancer capacity over approximately 20 cancers types *in vitro*. Among these cancer cell lines, brain cancer, skin cancer, breast cancer, colorectal cancer, lung cancer, cervical cancer, leukemia, and hepatoma, as well as head & neck cancer have been intensively investigated [Fig. 1(c)] Refs. 39, 102–105 and references therein. The first *in vivo* demonstration of LTP anti-cancer potential was done by Vandamme *et al.*[106] Human U87 glioblastoma xenotransplants were used in that study. Tumor volume measurements performed 24 h after the end of the treatment course revealed a significantly lower tumor volume in the treated group compared to control. It was argued that the observed effects are related to ROS-mediated apoptosis. Follow up studies by various investigators achieved similar results that the growth of tumor *in vivo* was significantly halted by LTP treatment on the skin of mice. For example, a study on a bladder tumor mouse xenograft through subcutaneous injection displayed a similar effect[107] [Fig. 27(a)]. After 24 h following a 2 min of LTP treatment, the treated tumor significantly decreased in size and could not be observed on the skin of mice.[107] Similar experiments were performed on a murine melanoma model which showed that tumor growth was completely inhibited over 3 weeks after LTP treatment [Fig. 27(b)]. The corresponding mice survival rates were also strongly increased compared with the control group without the LTP treatment.

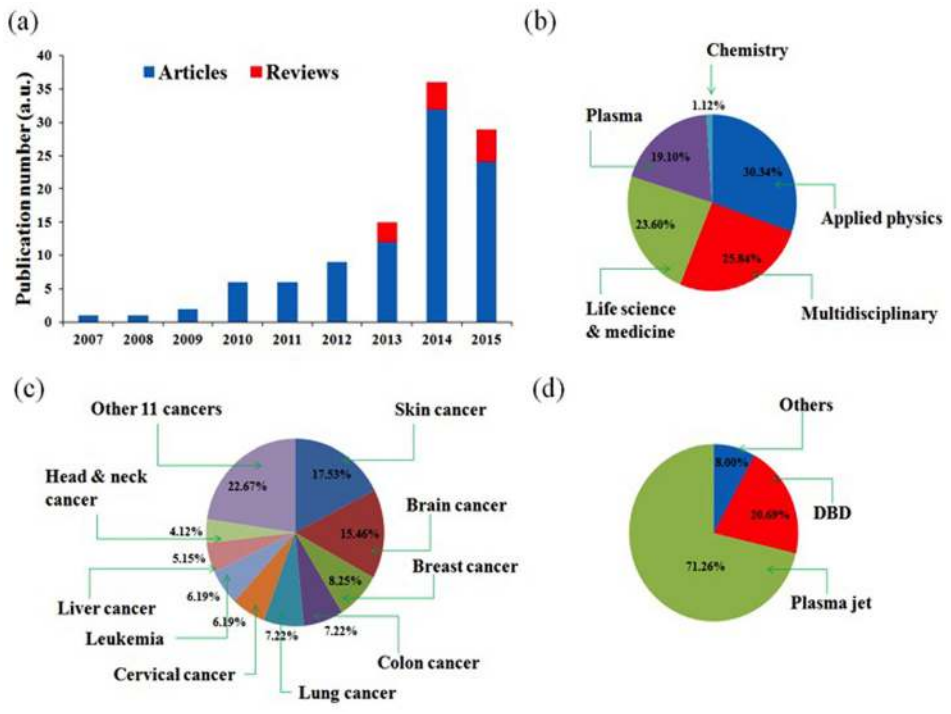

FIG. 26. The research status of the application of LTP on cancer treatment by 2016. (a) Publication number; (b) The journal types of articles; (c) Cancers in articles; (d) Plasma devices in articles. From Ref. 102.

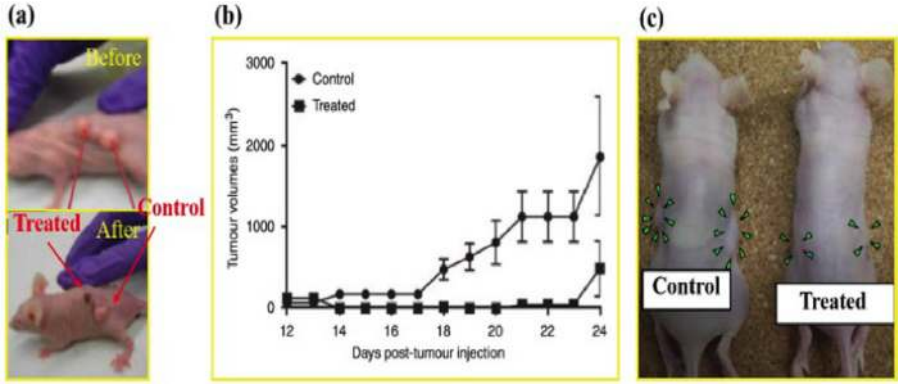

FIG. 27. The anti-cancer effect of LTP in **the** mice model. (a) Image of mouse with two tumors before and after the plasma jet treatment for 24 h. The subcutaneous tumors are grown from the seeded bladder cancer cells (SCaBER). From Keidar *et al.*;[107] (b) Cold plasma treatment effect on the growth of established tumor in a murine melanoma model from Keidar *et al.*,[107] (c) Images of nude mice bearing subcutaneous NOS2TR tumors before and after the injection of the cold plasma-stimulated medium. Green arrowheads indicate the tumor site. From Utsumi *et al.*, PLoS One **8**, e81576 (2013).

A very recent study on the anti-melanoma effect of plasma further confirmed that the LTP-treated melanoma tissue completely disappeared on the 22nd day after the treatment.[108] One promising candidate is that LTP treatment activates the immune response *in vivo* to attack the tumor.[109–111] The macrophages can be activated *in vitro* by a uniform nanosecond pulsed DBD (nspDBD) and improves the healing effect of an artificial wound. The uniform nspDBD also enhanced the anti-tumor effects through both the induction of immunogenic cell death in tumor cells and augmentation of macrophage's function. In a recent review, Miller *et al.* provided a comprehensive introduction on the promising cancer immunotherapy based on LTP treatment.[109] By optimizing the parameters of LTP to induce immunogenic cell death in tumors locally, it is possible to trigger specific, protective immune responses systematically.

B. Antimicrobial effect of plasma and plasma mediated wound healing

As mentioned earlier, the first biological application of LTP was about the inactivation of bacteria on biotic and abiotic surfaces and in media.[9,112] In addition, LTP was found to be effective in treatment of biofilms and wound surfaces.[113,114] Overall, Gram-negative bacteria were more susceptible to plasma treatment than Gram-positive bacteria. A rat model of a superficial slash wound infected with *P. aeruginosa* and the plasma-sensitive *Staphylococcus aureus* strain Sa 78 was used to assess the efficiency of argon plasma treatment. A 10 min treatment significantly reduced bacterial loads on the wound surface. A 5-day course of daily plasma treatments eliminated *P. aeruginosa* from the plasma-treated animals 2 days earlier than from the control ones. A statistically significant increase in the rate of wound closure was observed in plasma-treated animals after the third day of the course. Overall, it can be concluded that there is considerable potential for non-thermal argon plasma in eliminating pathogenic bacteria from biofilms and wound surfaces. A recent study concluded that treating cells with cold plasma leads to their regeneration and rejuvenation. This result can be used to develop a plasma therapy program for patients with non-healing wounds.[114,115]

It is important to note here that in addition to the experimental work there were some attempts at modeling and simulation of the interaction between LTP and tissues.[116,117] Modeling work is very valuable and there is a need for this to be pursued more vigorously in the future.

C. Low temperature plasma in dentistry

Low temperature plasma can be used to fight periodontal diseases and to inactivate oral borne bacteria. The antibacterial efficacy of LTP was assessed against several types of bacteria of relevance to dental applications, including *Enterococcus faecalis*.[118–120] As an illustrative example, inactivation experiment results show that LTP can efficiently kill *Enterococcus faecalis*, one of the main types of bacterium causing failure of root-canal treatment, in several minutes. The experiments were performed with the root canal model both in *wet* (root canal filled with a bacterial suspension) and in *dry* (root canal contaminated and dried) conditions. It was shown that the direct treatment under dry conditions turned out to be the most effective, leading to a bacterial load mean reduction of 4.1.[120]

D. HIV (virus) treatment by LTP

LTP can inactivate viruses.[121] Very recently, the effects of CAP on HIV-1 replication in monocyte-derived macrophages (MDM) were studied.[122] It was demonstrated that pre-treatment of infected cells with LTP reduced levels of CD4 and CCR5, inhibiting virus-cell fusion, viral reverse transcription, and integration. In addition, LTP pre-treatment affected cellular factors required for post-entry events, which bypasses HIV receptor-mediated fusion at the plasma membrane during entry, was also inhibited. Virus particles produced by LTP-treated cells had reduced infectivity, suggesting that the inhibitory effect of LTP extended to the second cycle of infection. Representative results shown in Fig. 28 demonstrate that treatment of the virus suspension with LTP significantly reduced the ability of this virus to establish infection in MDM. These results have been reproduced with infected cells from 6 different donors. This effect of LTP could be due to damage to the viral envelope, which

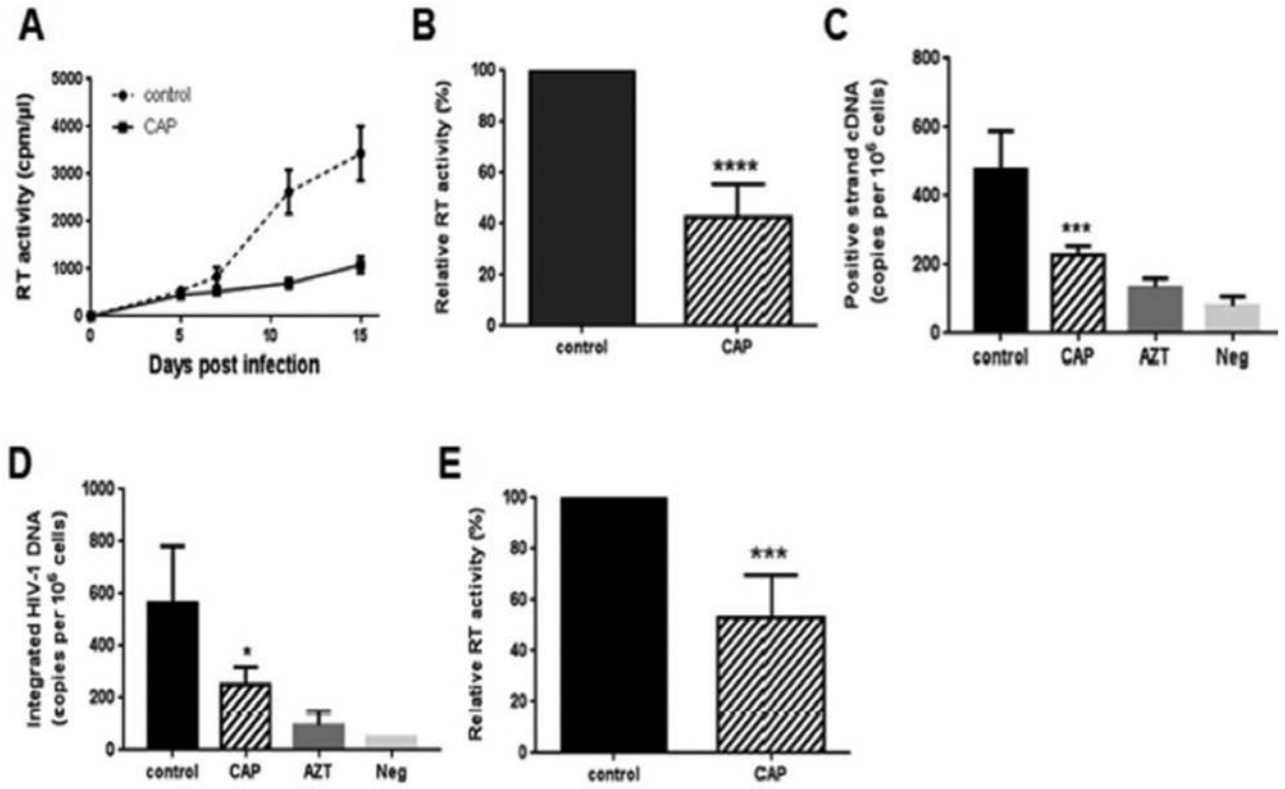

FIG. 28. LTP effects on HIV-1 replication. (a) Monocyte-derived macrophages treated with LTP or helium (control) were infected with HIV-1 ADA and viral replication was monitored for 15 days by RT activity in the culture supernatant; (b) Results are presented for RT analysis on day 15 after infection (performed as in panel a) for 7 different donors; (c) MDM infected with HIV-1 ADA; (d) HIV infected MDM were analyzed 48 h post-infection by Alu-GAG qPCR for integrated proviral DNA; **E.** HIV-1 ADA was treated with CAP or helium (control) and used to infect MDM. Virus infection was assessed by measuring reverse transcriptase activity in culture supernatant on day 10 ± 15 post-infection. From Volotskova *et al.*[122]

prevented virus-cell fusion, or destruction of the viral capsid leading to impairment of reverse transcription.

E. LTP processing of biocompatible materials

Low-temperature plasmas have been used as a tool for improving the surface interactions between materials and biological systems in various applications. Plasma processing in the health-care/biomaterials domain is currently experiencing spectacular growth.[123] This includes a wide range of applications such as functionalized surfaces for the enhanced adhesion of living cells; non-fouling coatings designed to completely inhibit *in vitro* adhesion of biomolecules, cells, bacteria, etc.; primer layers for the immobilization of peptides, enzymes, antibodies, and other types of biomolecules; etching processes for the fabrication of bio-MEMS (micro-electro mechanical systems); and "smart" drug-release systems.[123]

F. Summary

When used at the right operating conditions, atmospheric pressure low temperature plasmas are "bio-tolerable," in the sense that they can be applied to living cells and tissues without causing thermal or electrical damage. The bio-actions of LTP are mediated via its reactive species, electric field, charged particles, and in some cases UV or VUV radiation. LTP effects range from the inactivation of pathogens including antibiotic resistant bacteria (such as MRSA), the enhancement of proliferation of healthy cells such as fibroblasts, and the destruction of aberrant cells such as cancer cells. Each of these effects can be achieved by selecting and controlling the relevant operating parameter of the plasma. Therefore, establishing controlled/controllable conditions is paramount in order to achieve the desired effects. However, before using LTP as a basis for a medical therapy it is crucial that the potential risks are known and in-depth studies of its safety, including cytotoxicity and genotoxicity, are fully researched.[124–126]

VI. PRESENT STATUS AND FUTURE OUTLOOK

Mounting evidence is showing that the effects of LTP on biological cells are mediated via the reactive oxygen and nitrogen species (ROS and RNS). However, charged particles and electric fields should not be discounted. High electric fields have been shown to cause electroporation which causes pores to open in the cell membrane. This can help the ROS and RNS enter the cells and cause internal reactions with organelles with devastating effects. In the case of bacteria, the reactive species that enter the cells can directly react with DNA which is not encased within a nucleus and is therefore vulnerable to direct chemical attack. In the case of cancer cells, which are under high oxidative stress, injection of additional ROS can overwhelm the cell defenses and causes the cells to undergo apoptosis. As for the charged particles generated by plasma, the following are the possibilities: 1. Charge build-up on the outer cell membrane can

change the membrane potential and/or cause electrostatic forces that can challenge the tensile strength of the membrane; 2. changing electric charge balance at the cell membrane by partially neutralizing positive charges associated with ion channels.

Some of the remarkable achievements of plasma medicine can be summarized as follows:

1. Inactivation of bacteria: with the rise of antibiotic resistant strains serious health challenges are on the rise. Nosocomial infections are causing a high level of mortality in patients with a compromised immune system. LTP was shown to be able to inactivate antibiotic resistant bacteria such as MRSA. So far, there have been no reports that bacteria can build up resistance to LTP exposure.
2. LTP has been shown to be able to help in the treatment of chronic wounds, such as diabetic ulcers, which could not be treated by other conventional therapies. LTP's actions are two-fold. One is the reduction of infection by killing a high number of bacterial cells infecting the wound. Second is the enhancement of proliferation of fibroblasts and angiogenesis.
3. LTP has shown excellent selectivity in killing cancer cells while not harming normal healthy cells. One of the hypotheses explaining this selectivity is that cancer cells exhibit much higher metabolic rates than normal cells and therefore are under high oxidative stress. Adding extra ROS to the cancer cells leads to apoptosis as the cells becomes unable to cope. However, other investigations showed that other mechanisms are in action, such cell as cycle arrest and/or activation of caspases that can end up in apoptosis.

As of the present many mechanisms of interaction of LTP with prokaryotic and eukaryotic cells have been elucidated. However, much more work and careful investigations are still needed in order to generate a coherent and complete picture. Amongst these are: 1. Accurate measurements of the concentrations and fluxes of the relevant species both in the gaseous and liquid phases; 2. Investigations of the role of the plasma-generated electric field which can open pores in the cell membrane; 3. Elucidation of the plasma-triggered biochemical pathways whereby apoptosis can occur in cancer cells; 4. Conduct more investigations on the effects of LTP on macromolecules such as DNA and proteins; 5. Identification of any possible long-term cytotoxic effects that LTP can cause to healthy cells; 6. Investigation of possible genotoxic effects, especially on healthy cells, since any such effects could have serious implications (such as mutation); 7. Figuring out what other possible effects plasma could induce in tissues and tumors, such as change in blood flow, variation in the oxygen level, etc.; 8. Assessing the extent of the impact of LTP exposure on the immune system.

In addition to empirical data, mathematical modeling of the interaction of LTP with biological cells and tissues needs to be further developed. One of the interesting approaches being investigated in the case of cancer applications is the use of plasma activated media (PAM) instead of direct plasma treatment. Many encouraging results have been reported by several groups using this modality. These studies require a good understanding of the interaction of plasma with liquids, a branch of plasma applications that is experiencing heightened interest and is being pursued both experimentally and computationally. One of the advantages of using PAM is that it can be stored for later use. Investigators have reported that PAM can remain efficacious in killing cancer cells even after several hours of storage.

At this juncture, plasma medicine seems to have a very encouraging outlook. Many important milestones have been achieved during the last two decades and the field has experienced exponential growth both in the quality and quantity of data and knowledge generated by a global research community. Plasma medicine seems to be at the stage when it is almost ready to move out of the research laboratory and enter into the health care arena. The involvement and collaborations with medical doctors and biology experts have been crucial to the remarkable advancement experienced by the field. In the near future, extensive clinical trials need to be carried out for a final push of this technology to be adopted as the basis of various medical therapies. These include wound healing, dentistry, oncology, and others.

[1]R. Mogul, A. A. Bolaposshakov, S. L. Chan, R. M. Stevens, B. N. Khare, M. Meyyappan, and J. D. Trent, Biotechnol. Prog. **19**, 776 (2003).
[2]A. A. Bol'shakov, B. A. Cruden, R. Mogul, M. V. V. S. Rao, A. P. Sharma, B. N. Khare, and M. Meyyappan, AIAA J. **42**, 823 (2004).
[3]K. R. Stalder, "Plasma characteristics of electrosurgical discharges," in *Proceedings of the Gaseous Electronics Conference, San Francisco, CA* (2003), p. 16.
[4]M. Moisan, J. Barbeau, S. Moreau, J. Pelletier, M. Tabrizian, and L. H. Yahia, Int. J. Pharm. **226**, 1 (2001).
[5]D. A. Drossman, N. J. Shaheen, and I. S. Grimm, "Argon plasma coagulation," in *Handbook of Gastroenterology* Procedures, 4th ed. (Lippincotts Williams & Wilkins, Philadelphia, 2005), p. 235.
[6]S. Kanazawa, M. Kogoma, T. Moriwaki, and S. Okazaki, J. Phys. D: Appl. Phys. **21**, 838 (1988).
[7]F. Massines, C. Mayoux, R. Messaoudi, A. Rabehi, and P. Ségur, in *Proceedings of the GD-92, Swansea, UK* (1992), Vol. **2**, p. 730.
[8]J. R. Roth, M. Laroussi, and C. Liu, in *Proceedings of the IEEE International Conference on Plasma Science* (1992), p. 170.
[9]M. Laroussi, IEEE Trans. Plasma Sci. **24**, 1188 (1996).
[10]A. B. Shekhter, R. K. Kabisov, A. V. Pekshev, N. P. Kozlov, and Y. L. Perov, Bull. Exp. Biol. Med. **126**, 829 (1998).
[11]E. Stoffels, A. J. Flikweert, W. W. Stoffels, and G. M. W. Kroesen, Plasma Sources. Sci. Technol. **11**, 383 (2002).
[12]M. Laroussi and T. Akan, Plasma Processes Polym. **4**, 777 (2007).
[13]X. Lu, M. Laroussi, and V. Puech, Plasma Sources Sci. Technol. **21**, 034005 (2012).
[14]M. Laroussi and X. Lu, Appl. Phys. Lett. **87**, 113902 (2005).
[15]K.-D. Weltmann, R. Brandenburg, T. Von Woedtke, J. Ehlbeck, R. Foest, M. Stieber, and E. Kindel, J. Phys. D: Appl. Phys. **41**, 194008 (2008).
[16]T. Du Moncel, *Notice sur l'appareil d'induction electrique de Ruhmkorff et sur les experiences que l'on peut faire avec cet instrument* (Hachette et Cie Publishers, 1855).
[17]W. von Siemens, Poggendorfs Ann. Phys. Chem. **12**, 66 (1857).
[18]A. Von Engel, R. Seelinger, and M. Steenbeck, Z. Phys. **85**, 144 (1933).
[19]U. Kogelschatz, Pure Appl. Chem. **62**, 1667 (1990).
[20]U. Kogelschatz, B. Eliasson, and W. Egli, J. Phys. IV **7**(C4), 47 (1997).
[21]U. Kogelschatz, IEEE Trans. Plasma Sci. **30**, 1400 (2002).
[22]R. P. Mildren and R. J. Carman, J. Phys. D: Appl. Phys. **34**, 3378 (2001).
[23]X. Duten, D. Packan, L. Yu, C. O. Laux, and C. H. Kruger, IEEE Trans. Plasma Sci. **30**, 178 (2002).
[24]M. Laroussi, X. Lu, V. Kolobov, and R. Arslanbekov, J. Appl. Phys. **96**, 3028 (2004).
[25]X. Lu and M. Laroussi, J. Phys. D: Appl. Phys. **39**, 1127 (2006).
[26]M. Laroussi and A. Fridman, Plasma Processes Polym. **5**, 501 (2008).
[27]G. Fridman, G. Friedman, A. Gutsol, A. B. Shekhter, V. N. Vasilets, and A. Fridman, Plasma Processes Polym. **5**, 503 (2008).

[28]M. Laroussi, IEEE Trans. Plasma Sci. **37**, 714 (2009).
[29]T. Yokoyama, M. Kogoma, T. Moriwaki, and S. Okazaki, J. Phys. D: Appl. Phys. **23**, 1125 (1990).
[30]F. Massines, A. Rabehi, P. Decomps, R. B. Gadri, P. Ségur, and C. Mayoux, J. Appl. Phys. **82**, 2950 (1998).
[31]S. Okazaki, M. Kogoma, M. Uehara, and Y. Kimura, J. Phys. D: Appl. Phys. **26**, 889 (1993).
[32]N. Gherardi, G. Gouda, E. Gat, A. Ricard, and F. Massines, Plasma Sources Sci. Technol. **9**, 340 (2000).
[33]M. Laroussi, I. Alexeff, J. P. Richardson, and F. F. Dyer, IEEE Trans. Plasma Sci. **30**, 158 (2002).
[34]N. Gherardi and F. Massines, IEEE Trans. Plasma Sci. **29**, 536 (2001).
[35]J. J. Shi, X. T. Deng, R. Hall, J. D. Punnett, and M. Kong, J. Appl. Phys. **94**, 6303 (2003).
[36]F. Massines, N. Gherardi, N. Naude, and P. Segur, Plasma Phys. Controlled Fusion **47**, B557 (2005).
[37]A. Schutze, J. Y. Jeong, S. E. Babyan, J. Park, G. S. Selwyn, and R. F. Hicks, IEEE Trans. Plasma Sci. **26**, 1685 (1998).
[38]M. Laroussi, C. Tendero, X. Lu, S. Alla, and W. L. Hynes, Plasma Proc. Polym. **3**, 470 (2006).
[39]N. Barekzi and M. Laroussi, Plasma Processes Polym. **10**, 1039 (2013).
[40]D. Graves, J. Phys. D: Appl. Phys. **45**, 263001 (2012).
[41]A. Shashurin, M. Keidar, S. Bronnikov, R. A. Jurjus, and M. A. Stepp, Appl. Phys. Lett. **93**, 181501 (2008).
[42]M. Keidar, A. Shashurin, O. Volotskova, M. A. Stepp, P. Srinivasan, A. Sandler, and B. Trink, Phys. Plasmas **20**, 057101 (2013).
[43]M. Laroussi, S. Mohades, and N. Barekzi, Biointerphases **10**, 029401 (2015).
[44]M. Teschke, J. Kedzierski, E. G. Finantu-Dinu, D. Korzec, and J. Engemann, IEEE Trans. Plasma Sci. **33**, 310 (2005).
[45]X. Lu and M. Laroussi, J. Appl. Phys. **100**, 063302 (2006).
[46]N. Mericam-Bourdet, M. Laroussi, A. Begum, and E. Karakas, J. Phys. D: Appl. Phys. **42**, 055207 (2009).
[47]B. L. Sands, B. N. Ganguly, and K. Tachibana, Appl. Phys. Lett. **92**, 151503 (2008).
[48]J. L. Walsh and M. G. Kong, Appl. Phys. Lett. **93**, 111501 (2008).
[49]Q. Xiong, X. Lu, J. Liu, Y. Xian, Z. Xiong, F. Zou, C. Zou, W. Gong, J. Hu, K. Chen, X. Pei, Z. Jiang, and Y. Pan, J. Appl. Phys. **106**, 083302 (2009).
[50]M. Laroussi and X. Lu, "Spatial and temporal behavior of a plasma bullet launched by a pulsed cold plasma device," in Proceedings of the IEEE Pulse Power Plasma Science Conference, Albuquerque, NM, June 2007.
[51]E. Karakas, M. Koklu, and M. Laroussi, J. Phys. D: Appl. Phys. **43**, 155202 (2010).
[52]G. V. Naidis, J. Phys. D: Appl. Phys. **44**, 215203 (2011).
[53]G. V. Naidis, J. Phys. D: Appl. Phys. **43**, 402001 (2010).
[54]J.-P. Boeuf, L. Yang, and L. Pitchford, J. Phys. D: Appl. Phys. **46**, 015201 (2013).
[55]M. Yousfi, O. Eichwald, N. Merbahi, and N. Jomma, Plasma Sources Sci. Technol. **21**, 045003 (2012).
[56]D. Breden, K. Miki, and L. L. Raja, Plasma Sources Sci. Technol. **21**, 034011 (2012).
[57]D. Breden, K. Miki, and L. L. Raja, Appl. Phys. Lett. **99**, 111501 (2011).
[58]E. Karakas and M. Laroussi, J. Appl. Phys. **108**, 063305 (2010).
[59]J. Jarrige, M. Laroussi, and R. Karakas, Plasma Sources Sci. Technol. **19**, 065005 (2010).
[60]Y. Sakiyama, D. B. Graves, J. Jarrige, and M. Laroussi, Appl. Phys. Lett. **96**, 041501 (2010).
[61]X. Pei, Y. Lu, S. Wu, Q. Xiaong, and X. Lu, Plasma Sources Sci. Technol. **22**, 025023 (2013).
[62]A. Shashurin, M. N. Schneider, and M. Keidar, Plasma Sources. Sci. Technol. **21**, 049601 (2012).
[63]A. Begum, M. Laroussi, and M. R. Pervez, AIP Adv. **3**, 062117 (2013).
[64]G. B. Stretenovic, I. B. Krstic, V. V. Kovacevic, A. M. Obradovic, and M. M. Kuraica, J. Phys. D: Appl. Phys. **47**, 102001 (2014).
[65]A. Sobota, O. Guaitella, and E. Garcia-Caurel, J. Phys. D: Appl. Phys. **46**, 372001 (2013).
[66]X. Lu, G. Naidis, M. Laroussi, and K. Ostrikov, Phys. Rep. **540**, 123 (2014).
[67]X. Lu, G. V. Naidis, M. Laroussi, S. Reuter, D. B. Graves, and K. Ostrikov, Phys. Rep. **630**, 1 (2016).
[68]P. Bruggeman, D. C. Schram, M. G. Kong, and C. Leys, Plasma Processes Polym. **6**, 751 (2009).
[69]Q. Xiong, A. Nikiforov, X. Lu, and C. Leys, J. Phys. D: Appl. Phys. **43**, 415201 (2010).
[70]P. Bruggeman, D. C. Schram, M. A. Gonzalez, R. Rego, M. G. Kong, and C. Leys, Plasma Sources Sci. Technol. **18**, 025017 (2009).
[71]S. Tsurubuchi, Chem. Phys. **10**, 335 (1975).
[72]G. R. Mohlmann, C. I. M. Beenakker, and F. J. De Heer, Chem. Phys. **13**, 375 (1976)
[73]K. Bartschat and V. Zeman, Phys. Rev. A **59**, R2552 (1999).
[74]A. Dasgupta, M. Blaha, and L. J. Giuliani, Phys. Rev. A **61**, 012703 (1999).
[75]I. Hutchinson, *Principles of Plasma Diagnostics* (Cambridge University Press, 1987), pp. 216–221.
[76]J. Torres et al., J. Phys. D: Appl. Phys. **40**, 5929 (2007).
[77]R. Konjevic and N. Konjevic, Spectrochim. Acta, Part B **52**, 2077–2084 (1997).
[78]X. Lu, S. Wu, J. Gou, and Y. Pan, Sci. Rep. **4**, 7488 (2014).
[79]M. N. Shneider and R. B. Miles, J. Appl. Phys. **98**, 033301 (2005).
[80]A. Shashurin, M. N. Shneider, A. Dogariu, R. B. Miles, and M. Keidar, Appl. Phys. Lett. **94**, 231504 (2009).
[81]A. Shashurin, M. N. Shneider, and M. Keidar, Appl. Phys. Lett. **96**, 171502 (2010).
[82]J. S. Foster, Proc. R. Soc. London, Ser. A **117**, 137 (1927).
[83]S. Wu and X. Lu, Phys. Plasmas **21**, 023501 (2014).
[84]Q. Xiong, A. Nikiforov, L. Li, P. Vanraes, N. Britun, R. Snyders, X. Lu, and C. Leys, Eur. Phys. J. D **66**, 281 (2012).
[85]R. Kienle, M. P. Lee, and K. Kohse-Höinghaus, Appl. Phys. B **63**, 403 (1996).
[86]A. Ershov and J. Borysow, J. Phys. D: Appl. Phys. **28**, 68 (1995).
[87]R. Ono and T. Oda, J. Phys. D: Appl. Phys. **35**, 2133 (2002).
[88]S. Yonemori, Y. Nakagawa, R. Ono, and T. Oda, J. Phys. D: Appl. Phys. **45**, 225202 (2012).
[89]G. Dilecce, P. F. Ambrico, M. Simek, and S. De Benedictis, Chem. Phys. **398**, 142 (2012).
[90]F. Tochikubo, S. Uchida, and T. Watanabe, Jpn. J. Appl. Phys., Part 1 **43**, 315 (2004).
[91]T. Verreycken, R. M. van der Horst, A. H. F. M. Baede, E. M. van Veldhuizen, and P. J. Bruggeman, J. Phys. D: Appl. Phys. **45**, 045205 (2012).
[92]X. Pei, S. Wu, Y. Xian, X. Lu, and Y. Pan, IEEE Trans. Plasma Sci. **42**, 1206 (2014).
[93]P. Chu and X. Lu, *Low Temperature Plasma Technology: Methods and Applications* (CRC Press/Taylor & Francis Group, 2014).
[94]A. Van Gessel, S. Van Grootel, and P. Bruggeman, Plasma Sources Sci. Technol. **22**, 055010 (2013).
[95]S. Reuter, J. Winter, A. Schmidt-Bleker, D. Schroeder, H. Lange, N. Knake, V. Schulz-von der Gathen, and K.-D. Weltmann, Plasma Sources Sci. Technol. **21**, 024005 (2012).
[96]Y. Sakiyama, N. Knake, D. Schroder, J. Winter, V. Schulz-von der Gathen, and D. B. Graves, Appl. Phys. Lett. **97**, 151501 (2010).
[97]Y. Yue, Y. Xian, X. Pei, and X. Lu, Phys. Plasmas **23**, 123503 (2016).
[98]M. Laroussi, M. Kong, G. Morfill, and W. Stolz, *Plasma Medicine: Applications of Low Temperature Gas Plasma in Medicine and Biology* (Cambridge University Press, Cambridge, UK, 2012).
[99]M. Keidar and I. I. Beilis, *Plasma Engineering: Application in Aerospace, Nanotechnology and Bio-Nanotechnology* (Elsevier, Oxford, UK, 2013).
[100]M. Keidar and E. Robert, "Preface to Special Topic: Plasmas for medical applications," Phys. Plasmas **22**, 121901 (2015).
[101]M. Keidar, Plasma Source Sci. Technol. **24**, 033001 (2015).
[102]D. Yan, J. Sherman, and M. Keidar, Oncotarget **8**, 15977 (2017).
[103]M. Laroussi, Plasma Processes Polym. **11**, 1138 (2014).
[104]J. Schlegel, J. Koritzer, and V. Boxhammer, Clin. Plasma Med. **1**, 2 (2013).
[105]H. Tanaka, M. Mizuno, K. Ishikawa, K. Takeda, K. Nakamura, F. Utsumi, H. Kajiyama, H. Kano, Y. Okazaki, S. Toyokuni, S. Maruyama, F. Kikkawa, and M. Hori, IEEE Trans. Plasma Sci. **42**, 3760 (2014).

[106]M. Vandamme, E. Robert, S. Dozias, J. Sobilo, S. Lerondel, A. Le Pape, and J.-M. Pouvesle, Plasma Med. **1**, 27 (2011).
[107]M. Keidar, R. Walk, A. Shashurin, P. Srinivasan, A. Sandler, S. Dasgupta, R. Ravi, R. Guerrero-Preston, and B. Trink, Br. J. Cancer. **105**, 1295 (2011).
[108]N. Chernets, D. S. Kurpad, V. Alexeev, D. B. Rodrigues, and T. A. Freeman, Plasma Processes Polym. **12**, 1400 (2015).
[109]V. Miller, A. Lin, and A. Fridman, Plasma Chem. Plasma Process. **36**, 259 (2016).
[110]A. Lin, B. Truong, A. Pappas, K. Kirifides, A. Oubarri, S. Chen, D. Dobrynin, G. Fridman, A. Fridman, N. Sang, and V. Miller, Plasma Processes Polym. **12**, 1392 (2015).
[111]V. Miller, A. Lin, G. Fridman, D. Dobrynin, and A. Fridman, Plasma Processes Polym. **11**, 1193 (2014).
[112]M. Laroussi, Plasma Processes Polym. **2**, 391 (2005).
[113]S. A. Ermolaeva *et al.*, J. Med. Microbiol. **60**, 75 (2011).
[114]G. Isbary, G. Morfill, H. U. Schmidt, M. Georgi, K. Ramrath, J. Heinlin *et al.*, Br. J. Dermatol. **163**, 78 (2010).
[115]E. Sysolyatina, M. Vasiliev, M. Kurnaeva, I. Kornienko, O. Petrov, V. Fortov, A. Gintsburg, E. Petersen, and S. Ermolaeva, J. Phys. D: Appl. Phys. **49**, 294002 (2016).
[116]N. Y. Babaeva, W. Tian, and M. J. Kushner, J. Phys D: Appl. Phys. **47**, 235201 (2014).
[117]A. Bogaerts, M. Yusupov, J. van der Paal, C. C. W. Verlackt, and E. C. Neyts, Plasma Processes Polym. **11**, 1156 (2014).
[118]X. Lu, Z. Jiang, Q. Xiong, Z. Y. Tang, and Y. Pan, Appl. Phys. Lett. **92**, 151504 (2008).
[119]A. D. Morris, G. B. McCombs, T. Akan, W. Hynes, M. Laroussi, and S. L. Tolle, J. Dent. Hyg. **83**, 55 (2009).
[120]E. Simoncelli, Clin. Plasma Med. **3**, 77 (2015).
[121]H. A. Aboubakr, U. Gangal, M. M. Youssef, S. M. Goyal, and P. J. Bruggeman, J. Phys. D: Appl. Phys. **49**, 204001 (2016).
[122]O. Volotskova, L. Dubrovsky, M. Keidar, and M. Bukrinsky, PloS One **11**(10), e0165322 (2016).
[123]R. d'Agostino, P. Favia, C. Oehr, and M. R. Wertheimer, Plasma Processes Polym. **2**, 7 (2005).
[124]A. Antoniu, T. Nakajima, H. Kurita, and A. Mizuno, J. Electrostat. **72**, 210 (2014).
[125]S. Kos, T. Blagus, M. Cemazar, G. Filipic, G. Sersa, and U. Cvelbar, PloS One **12**(4), e0174966 (2017).
[126]H. Kurita, S. Miyachika, H. Yasuda, K. Takashima, and A. Mizuno, Appl. Phys. Lett. **107**, 263702 (2015).